DUAL PLANISPHERES: AN APPROACH TO TEMPORAL AND GEOGRAPHIC GENERALITY IN INDIAN AND SOUTHEAST ASIAN ASTRONOMICAL TRADITIONS

Peeravit Koad
Center of Geosocial and Cultural Research for Sustainable Development (GSCR), Informatics Innovation Center of Excellence (IICE), and School of Informatics, Walailak University, Thaiburi, Thasala, Nakhon Si Thammarat 80160, Thailand.
E-mail: harrykoad@gmail.com

Kannattha Chaisriya*
Informatics Innovation Center of Excellence (IICE) and School of Informatics, Walailak University, Thaiburi, Thasala, Nakhon Si Thammarat 80160, Thailand.
*Author for correspondence.
E-mail: csomjit@wu.ac.th

Orapin Riyaprao
National Astronomical Research Institute of Thailand (NARIT), Don Kaeo, Mae Rim, Chiang Mai 50180, Thailand.
E-mail: orapin@narit.or.th

Cherdsak Saelee
Department of Physics and Materials Science, Faculty of Science, Chiang Mai University, Suthep, Mueang Chiang Mai, Chiang Mai 50200, Thailand.
E-mail: cherdsak.s@cmu.ac.th

and

Lester Gilbert
Faculty of Engineering and Physical Sciences, University of Southampton, University Road, Southampton, SO17 1BJ, United Kingdom.
E-mail: lg11@soton.ac.uk

Abstract: This study proposes a dual planispheric system consisting of an ecliptic–equatorial planisphere and an equatorial–horizontal planisphere to address long-standing temporal and geographic constraints inherent in traditional planispheric instruments. By separating celestial representation, precessional adjustment, and horizon dependent transformation into two complementary analog devices, the system enables geometric analysis of rising and setting phenomena across wide ranges of epoch and latitude without numerical computation. The rotate-and-read workflow is demonstrated through applications to stellar horizon phenomena, calendrical transitions, and architectural orientation in Indian and Southeast Asian contexts. Case studies involving Phanom Rung, solar New Year festivals, and the distinction between true and mean solar motion show close agreement with modern numerical simulations while retaining historically meaningful reference frames. The results indicate that the dual planispheres provide a transparent and reproducible framework for archaeoastronomical research and offer significant pedagogical value by making coordinate transformation, precession, and horizon geometry directly accessible through physical manipulation.

Keywords: Planisphere; axial precession; positional astronomy; archaeoastronomy; horizon phenomena.

1 INTRODUCTION

Planispheric instruments, most notably the planisphere and the astrolabe, have long occupied a central place in the history of astronomy as analog devices mediating between mathematical models of the heavens and observational practice. The mathematical foundations were laid in ancient Greek astronomy, and the concepts developed into mature instruments traditional to the Islamic world that later were transmitted into Medieval and Renaissance Europe. There these devices functioned as computational tools, pedagogical models, navigational aids, and cultural artifacts (Morrison, 2013; Safiai et al., 2017). By employing planar projections of the celestial sphere, they enabled users to address problems of timekeeping, calendrical reckoning, navigation, and religious observance, while also serving as prestige objects within scholarly and courtly contexts (Bentley, 2018; Moyer, 1999).

Despite their historical importance and enduring pedagogical value, traditional planispheric instruments are constrained by structural limitations that restrict their applicability be-

yond narrow temporal and geographic contexts. These constraints are not incidental design flaws but arise from the fundamental geometric challenge of representing three-dimensional celestial motion on a two-dimensional surface. As a result, historical planispheres and astrolabes necessarily embed specific assumptions about epoch, observer's latitude, and coordinate transformation within a single physical device. While such assumptions were appropriate for everyday astronomical practice within limited spatial and temporal horizons, they pose significant obstacles for modern research contexts that require systematic comparison of sky configurations across millennial timescales and widely separated geographic locations.

Two interrelated limitations are particularly consequential, the first of which is temporal. Historical planispheric instruments encode the sky in a fixed equatorial framework tied to a specific reference epoch, so axial precession progressively shifts the celestial poles and equinoxes, and produces increasing divergence between embedded star charts and the observed sky (Liu et al., 2022; Morrison, 2013; Nothaft, 2017; Strano, 2017). This limitation reflects a more fundamental geometric constraint. A fully reversible transformation among the ecliptic, equatorial, and horizontal coordinate systems cannot be achieved with a two-dimensional planisphere possessing only one rotational degree of freedom (Calabretta and Greisen, 2002; Jenkins, 2012; Müller, 2015). Consequently, modern planispheres continue to model the sky at a fixed latitude and reference epoch, most commonly J2000.0, implementing only the equatorial–horizontal transformation while stellar positions remain fixed (Bizouard and Cheng, 2023; Morris et al., 2018). As a result, axial precession is not represented explicitly, applicability is limited to roughly ±100 years, and these instruments fall short of the requirements of archaeoastronomy, ethnoastronomy, and astronomical heritage studies (Aterini, 2019; Longair, 2021; Seidelmann and Gurfil, 2016).

The second limitation is geographic. Most planispheric instruments incorporate the local horizon geometry directly into their design, typically fixing the instrument to a single terrestrial latitude (King, 2019). When such instruments are used at other latitudes, distortions arise that cannot be corrected through simple adjustment. Although early instrument-makers occasionally attempted partial remedies through interchangeable plates or correction tables, these solutions were inherently limited in spatial scope and analytical flexibility (Gessner, 2024). Consequently, traditional planispheric instruments cannot support systematic comparison of celestial phenomena as observed from different geographic regions.

Although historical efforts such as the *Saphea Arzachelis* sought to extend planispheric usability across multiple latitudes, these designs function as spherical analog devices rather than true planispheres and address geographic generality at the cost of analytical simplicity (Morrison, 2007). They do not accommodate axial precession or long-term celestial change. A modern precession planisphere developed by Dr. Dominic Ford in 2009 (https://in-the-sky.org/precession/) addresses a different limitation by visualizing axial precession for educational purposes. However, it lacks the historically grounded sidereal reference frames and culture specific epoch conventions required for the long-term astronomical analysis (Komonjinda et al., 2020; Pai and Shylaja, 2016; Riyaprao et al., 2023).

These limitations are particularly consequential for archaeoastronomy, ethnoastronomy, and astronomical heritage studies, where researchers seek to reconstruct the appearance and orientation of the sky across extended temporal intervals and diverse geographic settings. Contemporary research often relies on digital simulations, numerical ephemerides, and GIS-based horizon models to account for precession, proper motion, and site-specific observation conditions (Jones, 2015; McCluskey, 2015). While such approaches are powerful, they differ cognitively from historical instrumental practice and can obscure the underlying spherical geometry and coordinate transformations that analog instruments make explicit (Finney, 2001). Material studies of navigational and astronomical artifacts further indicate that historical practitioners relied on tangible instruments to mediate directly between celestial reference frames and observational contexts (Castro et al., 2015; Smith, 2002).

In response to these limitations, this study proposes a dual planispheric system that decomposes celestial transformation into two complementary stages, distributing stellar representation, precessional correction, and horizon-dependent behavior across two two-dimensional planispheres rather than a single instrument. The Precessional Planisphere (PP) represents the axial precession of the Earth operating within the ecliptic–equatorial framework and enables examination of sky configurations across approximately ±12,500 years by simple rotation. The Rotational Planisphere (RP) represents the rotation of the Earth operating within the equatorial–horizontal framework and functions as a latitude-independent geometric transformer by restricting output to

rising and setting phenomena. This separation reflects a principled response to geometric constraints and does not significantly limit cultural astronomical analysis, which often focuses on horizon-related phenomena and their cultural significance.

2 LITERATURE REVIEW

This Section establishes the theoretical foundations, design rationale, and historical context of the proposed dual planispheres. It identifies the geometric constraints and historical design choices that limit existing planispheric instruments and explains why no prior design has achieved both temporal scalability and geographic generality. This Section also outlines the temporal and geographic conventions we adopted to ensure that the PP and RP remain usable across extended time ranges and diverse observing locations.

2.1 Properties of the Astrolabe and the Planisphere

2.1.1 Form Factors

The planispheric astrolabe is traditionally a single-sided instrument, reflecting its historical use by mariners who predominantly navigated in the Northern Hemisphere. As a result, it provides incomplete representation of the southern celestial hemisphere and makes Southern Sky interpretation more difficult due to increased distortion toward that region (Zotti, 2008). Modern planispheres exist in both single-sided formats similar to the astrolabe and double-sided formats that separate the Northern and Southern Skies onto opposite sides. The double-sided planisphere offers more complete detail for both hemispheres without concentrating distortion at one celestial pole (Zotti et al., 2021). However, it consumes both sides of the instrument and thus precludes allocating the reverse side to additional astronomical surveying functions. By contrast, the reverse side of the astrolabe can be repurposed for other surveying and observational functions when used with an alidade, for example as a quadrant for measuring the altitude of celestial objects (Morrison, 2007). In this study, the proposed PP and RP are not intended to serve as multipurpose surveying instruments, and they are therefore designed as double-sided planispheres in order to reduce distortion.

2.1.2 Materials Used

Surviving planispheric astrolabes are commonly fabricated from metals such as brass for durability and aesthetic qualities (Davis and Lowne, 2015). Modern planispheres are typically produced from cardboard, which are easy to construct manually but less durable, or plastic sheets, which are more durable but more challenging to manufacture. Although metal is generally more durable than plastic, it is substantially heavier, whereas cardboard is vulnerable to moisture and damage in rainy conditions. These constraints make both metal and cardboard less practical for field use and portability (Zotti, 2008). Plastic, or a laminated structure in which cardboard is enclosed by plastic layers on both sides, is therefore considered the most suitable material for both the PP and RP in this study.

2.1.3 Number and Ordering of Plates

The planispheric astrolabe is designed for use at multiple latitudes by separating the horizontal coordinate component into two parts, the mater, which serves as the base and includes a time scale ring or limb, and a set of interchangeable plates engraved with horizontal coordinate grids for different latitudes (Gislén and Evans, 2024). To operate at a particular latitude, the corresponding plate, or the closest available latitude, can be inserted and placed on top of other plates. In contrast, modern planispheres typically fix the horizontal coordinate grid in place with a central rivet or metal pin, making it non-interchangeable. Another important difference concerns layer ordering. In the astrolabe, the latitude plate is placed beneath the rete or perforated star chart, whereas many modern planispheres place the horizontal coordinate grid overlay above the star chart disk (Zotti, 2008). When the grid is printed on transparent plastic, the overlaid lines can obscure stars underneath. Accordingly, the PP and RP follow the astrolabe layering principle by placing the coordinate grid beneath a transparent star chart.

2.1.4 Coordinate Projections

The planispheric astrolabe employs stereographic projection, in which the principal coordinate grid curves are circular arcs, a feature that facilitated construction with a compass in antiquity (Aterini, 2019). Modern planispheres also employ azimuthal equidistant projection, in which declination circles are concentric with uniform radial spacing from the center and other grids are non-circular arcs typically generated computationally. Given contemporary user familiarity, stereographic projection is often perceived as producing greater distortion at regions far from the projection center than azimuthal equidistant projection (Calabretta and Greisen, 2002). For this reason, both the PP and RP in this study are designed using azimuthal equidistant projection, which is readily implemented with computer-aided construction.

2.1.5 Additional Rulers

Both the PP and RP developed in this study incorporate a measurement scale analogous to the regula mounted on the front of an astrolabe, but absent in most modern planispheres (Morrison, 2007). The scale is expressed in polar coordinates, with parallels encoded as a radial linear scale and meridians as an angular scale. For the PP, it enables measurement of ecliptic longitude and latitude, while for the RP it enables measurement of right ascension and declination. Unlike the astrolabe's regula, which can measure declination only, the polar scale supports both coordinate pairs and is expected to be particularly useful for transferring stellar right ascension and declination at a specified epoch, as read from the PP, onto the RP. This transfer facilitates accurate determination of azimuth and rise and set times across different latitudes.

2.2 Astronomical Reference Systems and Time Conventions

This section defines the astronomical reference systems and temporal conventions adopted in the PP and RP. Stellar coordinates, calendar mapping, and time representation are specified relative to fixed reference epochs to provide a consistent framework for visualizing long term variations in sky orientation.

2.2.1 Ecliptic Coordinate System

In the PP, stellar coordinates are initially referenced to epoch J2000.0 and drawn from the SKY2000 Master Catalog, Version 5, Revision 4, produced within the SKYMAP Star Catalog System (Myers et al., 2015). The SKY2000 Master Catalog effort was originally developed for NASA spacecraft acquisition and attitude determination (guidance) applications (Warren, 2001). For the purposes of this study, the dataset is restricted to stars brighter than apparent magnitude 5.0, corresponding approximately to the limit of unaided human vision. The 88 constellation figures follow the IAU-designated convention (International Astronomical Union, 2022) to maintain familiarity for the international astronomical community and to ensure straightforward cross-referencing with modern star charts.

The ecliptic adopted in the PP is defined with respect to the J2000.0 reference epoch. Because the orientation of the ecliptic plane depends on the Earth's orbital parameters, which vary slowly over time due to planetary perturbations, fixing the ecliptic to J2000.0 provides a reference frame that allows axial precession to be visualized independently. However, because the long-term secular evolution of the orbital plane is not modeled, this introduces a small but cumulative inaccuracy when extrapolated far from the reference epoch. Consequently, the PP provides its highest geometric fidelity near AD 2000, and ecliptic longitudes and derived quantities at increasingly remote epochs should be interpreted as schematic approximations rather than precise physical values.

To visualize axial precession within the PP, the initial J2000.0 equatorial coordinates of these stars must be transformed into a static ecliptic coordinate system. This requires distinguishing between two reference points that correspond to dynamic and fixed frames of reference. The Vernal Equinox (VE) is defined by the intersection of the ecliptic with the celestial equator, and because the celestial equator precesses, the VE slowly drifts along the ecliptic (Capitaine and Wallace, 2006; Müller, 2015; Nothaft, 2017). Coordinate boundaries tied to this origin therefore shift relative to the stellar background. By contrast, the First Point of Aries (FPA) is a fixed origin defined by adopting the VE at a specified epoch and holding that zero-point constant with respect to the stars.

In this study, the PP is instantiated using a FPA-based ecliptic framework aligned with Classical Indian and Southeast Asian astronomical conventions. This instantiation is presented as an illustrative example, while the same planispheric architecture may be configured for alternative cultural traditions by adopting different epoch conventions, longitude origins, and stellar division schemes.

To align the PP with Classical Indian and Southeast Asian astronomical traditions, which often rely on a static ecliptic coordinate framework, the moving VE is treated here as the origin of the *sāyana system* (from Sanskrit *sa-* + *ayana*: with precession), while the fixed FPA is treated as the origin of the *nirāyana system* (from Sanskrit *nir-* + *ayana*: without precession), taken in this study as the VE at J500.0 (Koad et al., 2025). This *nirāyana ecliptic* framework is treated here as the source coordinate system for subsequent transformations to equatorial and horizontal coordinates. Within this framework, the PP adopts the Vedic nomenclature of the 12 *rāśis* (Indian zodiac signs) rather than Western zodiacal naming conventions (Table 1), and it incorporates the 27 *nakṣatras* (Indian lunar mansions) (Table 2). The *nakṣatra* groupings are not reproduced verbatim from the *Vedāṅga Jyotiṣa* or *Sūrya Siddhānta* (Burgess, 1935; Sastri, 1931). Instead, selected asterisms are adjusted so that their representative positions lie closer to the ecliptic and more closely approximate the angular spacing of the

lunar mansions as used in practice.

Stellar positions from the SKY2000 Master Catalog are first transformed into *nirāyana* ecliptic coordinates. Axial precession, excluding nutation, is incorporated using the general precession in ecliptic longitude reported by Capitaine et al. (2003), which at epoch J2000.0 is approximately 5,028.796195 arcseconds per Julian century, equivalent to about 71.59 years per degree. Applying this rate allows the PP to operate over the interval from 10,500 BC to AD 14,500 (±12,500 years from AD 2000), spanning nearly the full axial precession cycle.

Proper motion and other corrections related to apparent displacement, including light aberration, topocentric parallax, and atmospheric refraction, are neglected in order to preserve a clear, first-order geometric visualization of long-term sky orientation. As a result, the derived stellar positions and horizon directions should be interpreted as schematic rather than metrological. Users requiring higher accuracy for specific epochs or observing sites, such as studies involving high proper motion stars, lunar or planetary near horizon phenomena, or terrain-dependent rise and set points, should therefore apply appropriate external corrections, including catalog-based proper motion, site-specific refraction, and horizon profile adjustments.

Table 1: The Vedic zodiac signs (*rāśis*) used in the PP, their Western zodiac equivalents, and the corresponding *nirāyana* ecliptic longitude span.

No.	Vedic Zodiac (*Rāśi*)	Western Zodiac	*Nirāyana* Ecliptic Longitude
1	*Meṣa*	Aries	0° to 30°
2	*Vṛṣabha*	Taurus	30° to 60°
3	*Mithuna*	Gemini	60° to 90°
4	*Karkaṭa*	Cancer	90° to 120°
5	*Siṃha*	Leo	120° to 150°
6	*Kaṇya*	Virgo	150° to 180°
7	*Tula*	Libra	180° to 210°
8	*Vṛścika*	Scorpius	210° to 240°
9	*Dhanus*	Sagittarius	240° to 270°
10	*Makara*	Capricornus	270° to 300°
11	*Kumbha*	Aquarius	300° to 330°
12	*Mīna*	Pisces	330° to 0°

In this study, stellar coordinates are transformed from the J2000.0 reference epoch into a fixed ecliptic coordinate framework referenced to the FPA. This configuration enables long term representation of axial precession while maintaining compatibility with classical Indian and Southeast Asian astronomical traditions.

2.2.2 Gregorian Calendar

The calendar system (months and days) on the PP follows a simplified Gregorian convention. For clarity and mechanical consistency, February is fixed at 28 days, yielding a 365-day civil

Table 2: The Vedic lunar mansions (*nakṣatras*) used in the PP, with each mansion's representative modern star or asterism and its *nirāyana* ecliptic longitude span.

No.	Lunar Mansion (*Nakṣatra*)	Modern Star/Asterism (Number of Stars)	*Nirāyana* Ecliptic Longitude
1	*Aśvinī*	α, β, λ Ari (3)	0° 0' to 13° 20'
2	*Bharaṇī*	35, 39, 41 Ari (3)	13° 20' to 26° 40'
3	*Kṛttikā*	Pleiades (6)	26° 40' to 40° 0'
4	*Rohiṇī*	ε, δ, γ, θ, α Tau (5)	40° 0' to 53° 20'
5	*Mṛgaśira*	ζ, ε, δ Ori (3)	53° 20' to 66° 40'
6	*Ārdrā*	γ Gem (1)	66° 40' to 80° 0'
7	*Punarvasu*	α, β, υ, ι Gem (4)	80° 0' to 93° 20'
8	*Puṣya*	δ, γ, η, θ Cnc (4)	93° 20' to 106° 40'
9	*Aśleṣā*	κ, λ, ε, μ Leo (4)	106° 40' to 120° 0'
10	*Maghā*	ο, α, η, γ, ζ, Leo (5)	120° 0' to 133° 20'
11	*Pūrva Phalguṇī*	δ, θ Leo (2)	133° 20' to 146° 40'
12	*Uttara Phalguṇī*	β, 93 Leo (2)	146° 40' to 160° 0'
13	*Hasta*	ε, ρ, c, η, γ, δ Vir (6)	160° 0' to 173° 20'
14	*Citrā*	α Vir (1)	173° 20' to 186° 40'
15	*Svāti*	ι Vir (1)	186° 40' to 200° 0'
16	*Viśākha*	α, β, γ, σ Lib (4)	200° 0' to 213° 20'
17	*Anurādhā*	ρ, π, δ, β Sco (4)	213° 20' to 226° 40'
18	*Jyeṣṭha*	σ, α, τ Sco (3)	226° 40' to 240° 0'
19	*Mūla*	κ, Q, υ, λ, G, ι, θ, η, ζ, μ, ε Sco (11)	240° 0' to 253° 20'
20	*Pūrva Aṣāḍha*	δ, ε Sgr (2)	253° 20' to 266° 40'
21	*Uttara Aṣāḍha*	α, ζ Sgr (2)	266° 40' to 280° 0'
22	*Śravaṇa*	γ, α, β Aql (3)	280° 0' to 293° 20'
23	*Dhaniṣṭha*	δ, γ, ι, θ, ζ Cap (5)	293° 20' to 306° 40'
24	*Śatabhiṣak*	ζ, γ, η, π Aqr (4)	306° 40' to 320° 0'
25	*Pūrva Bhādrapadā*	α, β Peg (2)	320° 0' to 333° 20'
26	*Uttara Bhādrapadā*	γ Peg, α And (2)	333° 20' to 346° 40'
27	*Revatī*	ζ Psc (1)	346° 40' to 0° 0'

year. The VE is mapped by defining 0° of the true ecliptic longitude of the Sun to correspond to 12:00 local mean solar time (local noon) on 20 March, aligned with the Sun's entry into the mean VE of a specified date. Other dates are mapped by applying the Equation of the Center at epoch J2000.0 using the Kepler's transcendental equation solver described in Koad et al. (2025).

2.2.3 Local Mean Solar Time

The solar time system on the RP is expressed in Local Mean Solar Time (LMST), divided into 24 equal hours, so that it can be applied at any terrestrial longitude without redesign. Users who require Coordinated Universal Time (UTC) or related temporal quantities can convert from LMST as needed. This convention is sufficient for approximating the timing of near-horizon astronomical phenomena at arbitrary latitudes and does not compromise the computation of sidereal time, hour angle, or right ascension within the intended level of geometric abstraction.

In this study, LMST is used as a practical civil time proxy rather than a full treatment of modern astronomical time scales. Conversions among UTC, Universal Time 1 (UT1), and uniform dynamical times such as Terrestrial Time (TT) and, where relevant, Barycentric Dynamical Time (TDB) are not implemented, and the epoch-dependent offset Delta T ($\Delta T = TT - UT1$) is not modeled. Such conversions are needed when comparing UTC timestamps, reconstructing eclipses or occultations using TT or TDB ephemerides, or achieving high precision timing for ancient astronomical phenomena affected by UT1 and ΔT. In these cases, users would apply an external ΔT model and the appropriate UT1 or UTC and TT (or TDB) transformations before interpreting results in absolute clock time.

3 MATERIALS AND METHOD

This section details the design and construction of the PP and RP, covering the physical assembly of the instruments, the geometric framework governing celestial coordinate transformations together with its operational realization through disk rotation, and the structural and graphical elements of each planisphere. The complete full-scale graphical layouts of both planispheres are provided as a downloadable supplementary PDF file formatted for direct printing and physical assembly.

The same assembly procedure is used for both the PP and RP, since the two instruments share an identical three-layer mechanical structure. The PP is used here as the illustrated exemplar for clarity.

3.1 The Assembling Procedures

Both the PP and RP are constructed as rotating planispheres with identical mechanical structures. Each instrument consists of three circular layers: two transparent outer disks and one opaque inner disk. These layers are joined at the center by a single fastener that allows free rotation of the inner disk relative to the outer disks (Figure 1).

In each planisphere, the outer transparent disks represent the source coordinate system, while the inner cardboard disk represents the target coordinate system. For the *rāśis* and *nakṣatras* used in the PP as outlined in Tables 1 and 2, the outer disks encode the J500.0 *nirāyana* ecliptic coordinate system and the inner disk encodes the equatorial coordinate system of a specified date. For the RP, the outer disks encode the equatorial coordinate system and the inner disk encodes the horizontal coordinate system. Each planisphere is divided into two hemispheres: the PP is separated by the ecliptic, and the RP by the celestial equator.

The assembling process is described below in sequential stages:

(1) Preparation and Printing: All graphic components should be printed using a color laser printer to minimize ink dissolution when exposed to moisture. The transparent outer disks must be made from heat resistant plastic sheet to avoid deformation or melting during laser printing. To protect the printed surfaces from external abrasion during use, the graphics on the transparent sheets are horizontally-mirrored before printing so that the printed side faces inward when assembled.

The inner rotating disk should be printed on a cardboard thick enough to resist tearing and warping. Printing both hemispheres on opposite sides of a single thick cardboard sheet may lead to angular misalignment between the Northern and Southern sides. To avoid this, it is recommended that one hemisphere be printed on one side of a thick cardboard sheet, while the opposite hemisphere is printed on the front side of a separate thinner paper. These two sheets can then be carefully aligned back-to-back and bonded using a water-resistant adhesive.

(2) Cutting and Shaping: All plastic and cardboard sheets must be cut into precise circular shapes. The use of a circular cutter is strongly recommended to ensure concentric edges and uniform diameter. Care should be taken to avoid trimming regions reserved for gripping or stabilizing the transparent sheets during rotation. After cutting, the edges of all disks should be inspected and trimmed as needed to remove

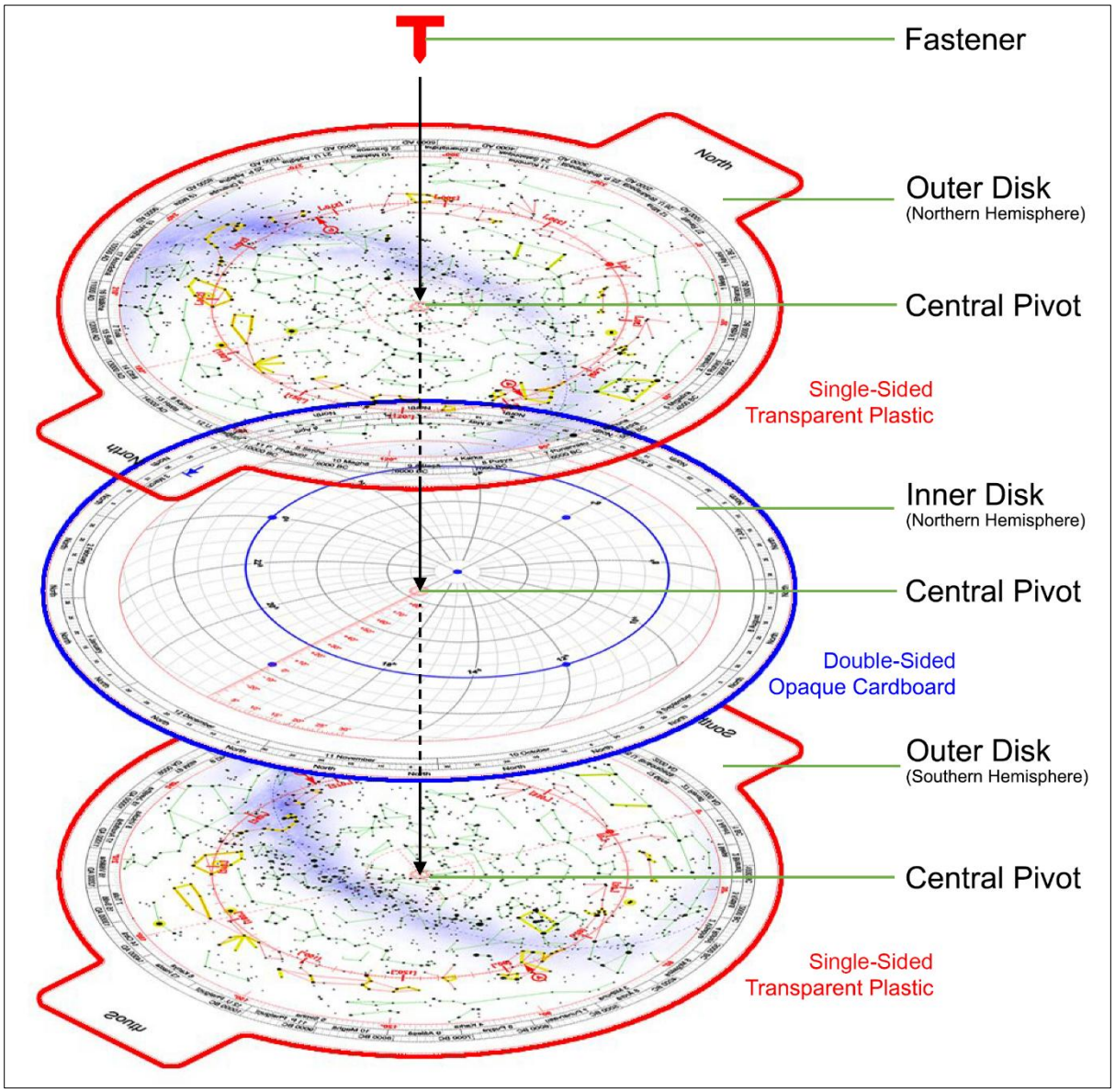


Figure 1: Schematic view of the structure and layer arrangement common to both the PP and RP. Each planisphere consists of three concentric disks aligned on a single central pivot secured by a fastener. Two single-sided transparent plastic outer disks encode the source coordinate system and separately represent the Northern and Southern Hemispheres. A double-sided opaque cardboard inner disk, placed between them, encodes the target coordinate system.

burrs or irregularities that could interfere with smooth rotation

(3) Alignment of Hemispheres: Each disk contains a central crosshair marking that defines the geometric center of the projection. Before fastening, all disks must be arranged into their correct hemispheric configurations and aligned by matching these crosshair markings on both the northern and southern sides. Drilling a small pilot hole at the crosshair location is recommended to improve alignment accuracy and ease of assembly.

(4) Final assembly: Once aligned, the disks are secured using a plastic or metal fastener inserted through the central hole. The fastener should be tightened only enough to hold the disks securely while still allowing the inner disk to rotate freely. Excessive force may cause angular misalignment or restrict rotation, reducing the usability of the instrument. After assembly, the rotation of the inner disk should be tested across the full range to ensure smooth motion and consistent alignment between the hemispheres.

3.2 Rotate-and-Read Coordinate Transformation

After assembly, the PP and RP enable geometric transformation between celestial coordinate systems through controlled relative rotation of

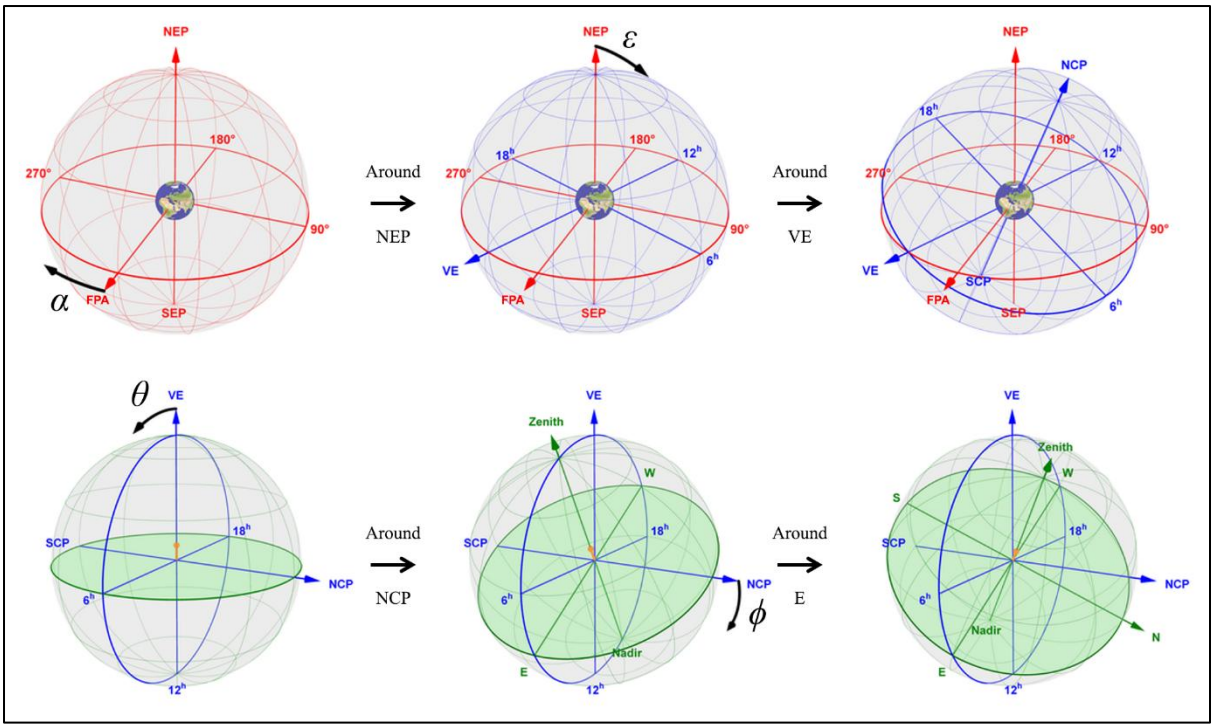


Figure 2 (Top): Transformation from the ecliptic to the equatorial coordinate system. First, the celestial sphere is rotated clockwise around the North Ecliptic Pole (NEP) by the precession angle (*ayanāṃśa*) α to separate the Vernal Equinox (VE) from the First Point of Aries (FPA). Next, the celestial sphere is rotated clockwise around the VE by the obliquity of the ecliptic ε to separate the North Celestial Pole (NCP) from the NEP. Bottom: Transformation from the equatorial to the horizontal coordinate system. First, the celestial sphere is rotated counterclockwise around the NCP by the angle of the local mean sidereal time θ to separate the zenith from the VE. Next, the celestial sphere is rotated clockwise around the East direction by the observer's geographic latitude ϕ to separate the North direction from the NCP.

their disks. These transformations correspond to standard spherical rotations of the celestial sphere and are implemented physically through the planispheric geometry, without recourse to explicit numerical computation. This mode of operation, termed Rotate-and-Read (R&R), is implemented in both the PP and the RP by rotating the respective disks into alignment and directly reading the resulting coordinate relationships from the overlaid grids.

The first R&R transformation from the *nirāyana* ecliptic coordinates at J500.0 to the equatorial coordinates of a specified date involves two instantaneous angular quantities: the precession angle called the *ayanāṃśa* α (defined as the signed angular separation from the FPA westward to the VE) and the obliquity of the ecliptic ε (Figure 2, top). In the PP, axial precession is represented by rotating the inner equatorial disk relative to the outer ecliptic disk by an angle corresponding to α for the specified year. The grid on the inner disk represents the equatorial grid rotated by a uniform ε having the value 23.439° at J2000.0 (Capitaine et al., 2003). Through this configuration, stellar positions expressed in *nirāyana* ecliptic coordinates are mapped directly onto their corresponding equatorial coordinates for the selected year.

The second R&R transformation from the equatorial coordinates at a given epoch to the horizontal coordinates involves two instantaneous angular quantities: the local mean sidereal time θ (defined as the angular separation from the observer's meridian Westward to the VE) and the observer's geographic latitude φ (Figure 2, bottom). In the RP, this transformation does not yield horizontal coordinates at a specified θ (or LMST) for a fixed latitude, but instead determines the rising and setting date and time of a star at any latitude. The grid on the inner disk represents the horizon geometry for all geographic latitudes, where the geographic latitude differs negligibly (no more than ±0.2°) from the GNSS provided geodetic latitude. Through this configuration, equatorial coordinates transferred from the PP and referenced on the outer disk are mapped onto their corresponding rising and setting conditions by rotating the inner disk until the stellar position intersects the Eastern or Western horizon for the selected latitude.

3.3 Description of Components and Elements of the PP

This part describes the assembled PP for the exemplar *nirāyana* source system in a systema-

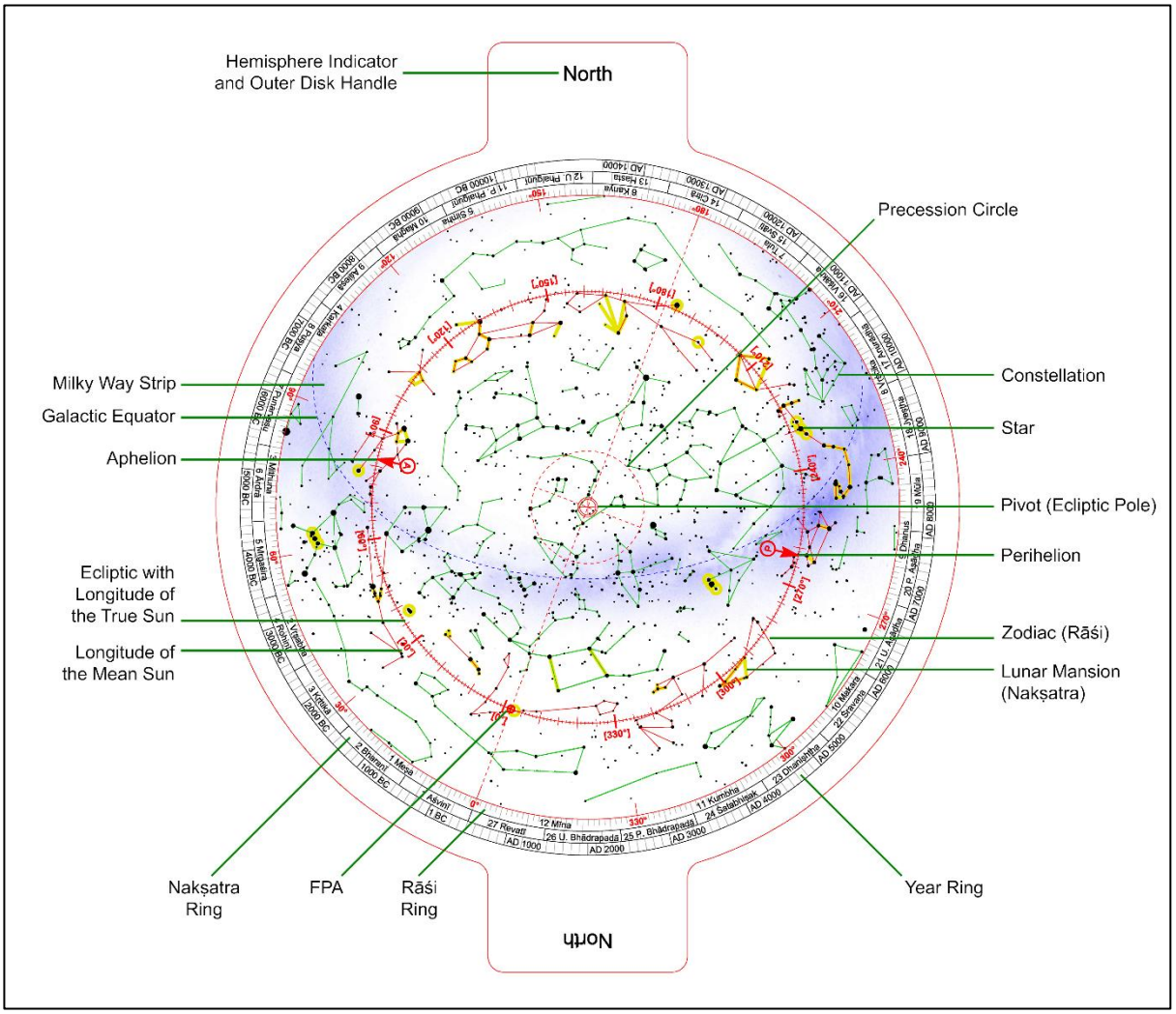


Figure 3: The Northern outer disk of the exemplar PP showing the *nirāyana* ecliptic star chart with *rāśi* and *nakṣatra* divisions, the ecliptic with the mean and true longitudes of the Sun, and the long-term year scale for visualizing axial precession.

tic manner. The PP is composed of three disk components: two transparent outer disks and one opaque inner rotating disk. Each component contains a set of printed elements, which are described below by proceeding from the outer disks toward the inner disk and, within each disk, from the central region outward to the outer edge. The outer disks of the PP, each produced from a reverse-printed transparent plastic sheet corresponding to one hemisphere, contain the following elements (Figure 3).

3.3.1 The Star Chart

Stars brighter than apparent magnitude 5.0 in both hemispheres in the *nirāyana* ecliptic coordinate system are plotted as black dots whose sizes scale with apparent magnitude on the uppermost graphical layer of the star chart. Constellation figures following IAU conventions are drawn beneath them using green lines, except for the zodiac figures along the ecliptic, which are drawn using thick red lines. Indian lunar mansions (*nakṣatras*), adapted from Classical Indian astronomical treatises, are also drawn beneath using thick yellow lines. The *rāśi* and *nakṣatra* overlays are included for this exemplar instantiation and are not intended to imply a unique mapping across all Indian and Southeast Asian traditions. The lowermost graphical layer represents the Milky Way band and the Galactic Equator, shown as a dashed blue curve.

3.3.2 The *Nirāyana* Ecliptic Circle

Drawn above the star chart, the ecliptic is represented by a red circle centered on the NEP or the South Ecliptic Pole (SEP), located at the central pivot. The ecliptic originates at the FPA, marked by a red circled cross symbol. The *nirāyana* ecliptic longitude of the fictitious mean Sun is indicated by tick marks with bracketed labels distributed along the ecliptic. These tick marks, computed from the Equation of the Center at epoch J2000.0 using the Kepler's trans-

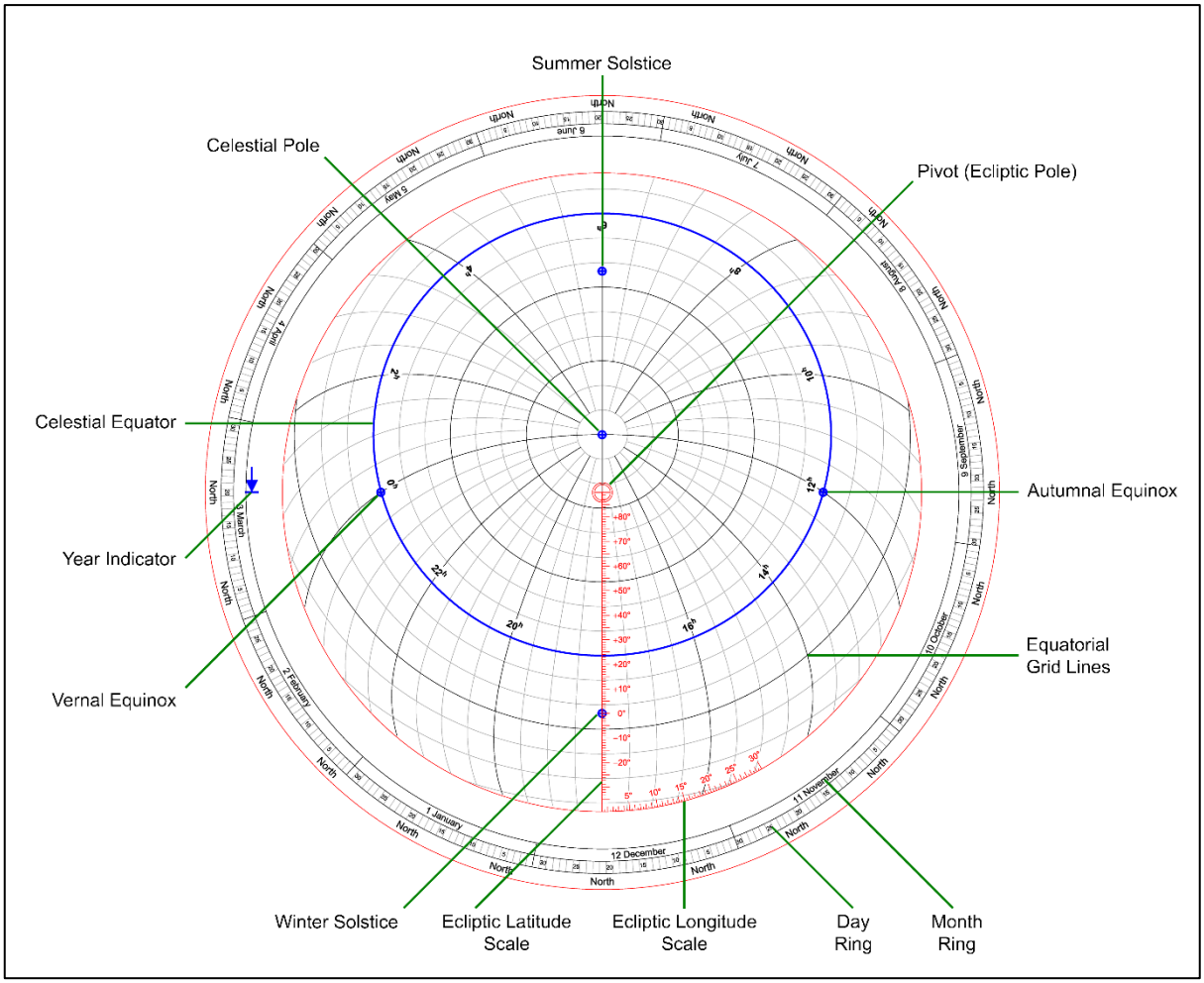


Figure 4: The Northern inner rotating disk of the exemplar PP displaying the equatorial coordinate grid, the Celestial Eequator with principal reference points, *nirāyana* ecliptic measurement scales, the year indicator, and the Gregorian Calendar ring.

cendental equation solver described in Koad et al. (2025), accompany the position of the true Sun as read using the *nirāyana* ecliptic longitude scale on the inner disk. True and mean ecliptic longitudes of the Sun are also used together with the calendar ring on the inner disk to determine calendrical reference dates, such as the day of *Meṣa Saṅkrānti* (the New Year's Day, when the true Sun reaches the FPA) of the Hindu solar calendar. The approximate positions of the Sun's perihelion at the *nirāyana* ecliptic longitude of 282.895° and the opposite aphelion are additionally marked on the ecliptic by the letters P and A enclosed in red arrowed circles.

3.3.3 *Rāśi* and *Nakṣatra* Rings

Near the outer edge of the outer disk, adjacent to the star chart area, a dual ring system encodes both the Indian zodiac signs and the lunar mansions. The inner ring divides the ecliptic into 12 equal segments of 30°, corresponding to the *rāśis* starting from the FPA (Table 1). The outer ring divides the ecliptic into 27 equal segments of 13° 20′, corresponding to the *nakṣatras* from *Aśvinī* to *Revatī* (Table 2). Together with the ecliptic longitude scale and the calendar ring on the inner disk, these rings support direct correspondence between sidereal divisions, ecliptic longitude, and calendrical reference.

3.3.4 Year Ring

The outermost ring, located next to the *rāśi* and *nakṣatra* rings, represents a Gregorian year scale spanning from 10,500 BC to AD 14,500. Major divisions are marked at 1,000-year intervals using black lines with numerals, while minor divisions at 100-year intervals are indicated by gray lines without numerals. This ring is used in conjunction with the year indicator on the inner disk to visualize axial precession across long temporal intervals.

The inner disk of the PP, printed with a hemisphere on each side, consists of the following components (Figure 4).

3.3.5 Equatorial Coordinate Grid

The innermost region contains the principal reference points and grid lines of the equatorial coordinate system. The VE, Summer Solstice (SS), Autumnal Equinox (AE), Winter Solstice (WS), NCP, and South Celestial Pole (SCP) are marked by red circled cross symbols. The Celestial Equator is represented by a thick blue circle encircling the NCP and passing through the VE and AE. When correctly aligned, the SS and WS marked on the inner disk coincide with their corresponding positions along the ecliptic on the outer disk. Right ascension and declination grid lines are drawn as black and gray curves surrounding the NCP and SCP.

3.3.6 *Nirāyana* Ecliptic Measurement Scales

An L-shaped group of *nirāyana* ecliptic measurement scales is provided on the inner disk. The ecliptic latitude scale is shown as a red linear scale with numerical labels extending from the NEP and SEP toward the outer edge of the disk. The *nirāyana* ecliptic longitude scale is shown as a red angular scale (spanning 0° to 30° for each *rāśi*) and is located near the outer edge of the disk beginning at the outer end of the ecliptic latitude scale. This longitude scale is used in conjunction with the *rāśi* and *nakṣatra* rings on the outer disk.

3.3.7 Year Indicator

The year indicator is shown as a blue line with a blue arrow to ensure clear visibility during use. It is positioned near the outer edge of the inner disk and is used together with the year ring on the outer disk to set the precessional offset for a selected year.

3.3.8 Calendar Ring

Located near the outer edge of the inner disk, adjacent to the equatorial grid, a pair of concentric rings shows the months and days of the 365-day Gregorian calendar. Together, these rings mark the approximate position of the true Sun along the J2000.0 ecliptic for any given date, computed using the Equation of the Center. They are used in conjunction with the *rāśi* and *nakṣatra* rings on the outer disk to support calendrical reference.

3.4 Description of Components and Elements of the RP

This part describes the components of the assembled RP in a systematic manner, following the same organizational principle as for the PP. Unlike the PP, the RP is not instantiated to a tradition-specific sidereal division scheme, and its outer disks are presented in a generally applicable equatorial framework. The description proceeds from the outer disks toward the inner disk, and within each disk from the central region outward to the outer edge. The outer disks of the RP, each produced from a reverse-printed transparent plastic sheet corresponding to one hemisphere, consist of the following components (Figure 5).

3.4.1 Equatorial Coordinate Grid

Superimposed on the outer disk is the equatorial coordinate grid. The celestial equator is represented by a thick blue circle located near the outer edge of the disk. Right ascension and declination grid lines are drawn in blue and light blue, extending from the NCP and SCP at the central pivot toward the celestial equator. Numerical labels for right ascension values are placed around the outer edge of the disk. This grid functions in conjunction with the equatorial measurement scales on the inner disk.

3.4.2 *Sāyana* Ecliptic Coordinate Grid

The outer disk also carries a reduced *sāyana* ecliptic coordinate grid intended for locating planetary positions. The ecliptic is represented by a red curve with tick marks indicating the true Sun on any date, accompanied by labeled *sāyana* ecliptic-longitude grid lines and ecliptic-latitude grid lines extending ±10° from the ecliptic. A reference *sāyana* ecliptic longitude arc at 0° is drawn as a red curve extending from the ecliptic near the outer edge of the disk toward the NEP and SEP.

3.4.3 Calendar Ring

Near the outer edge of the outer disk, a dual Gregorian calendar ring is provided. Unlike the calendar ring on the inner disk of the PP, this ring on the outer RP is divided into equally-spaced day slots to enforce the conventionally-used LMST. The irregularity of Earth's orbit, which gives rise to the Equation of the Center, is accounted for in the ecliptic tick marks. This calendar ring is used in conjunction with the time ring on the inner disk to relate calendar dates to LMST within the RP framework.

The inner disk of the RP, printed on opaque cardboard and assembled as a double-sided disk corresponding to both hemispheres, consists of the following components (Figure 6).

3.4.4 Horizontal Coordinate Grid

The inner disk encodes the horizontal coordinate system as a set of horizon curves corresponding to all geographic latitudes together with rising and setting azimuth grids. Horizon curves are drawn as horizontal curves that converge at the Eastern and Western points, spanning from the horizon at the South Pole through the ter-

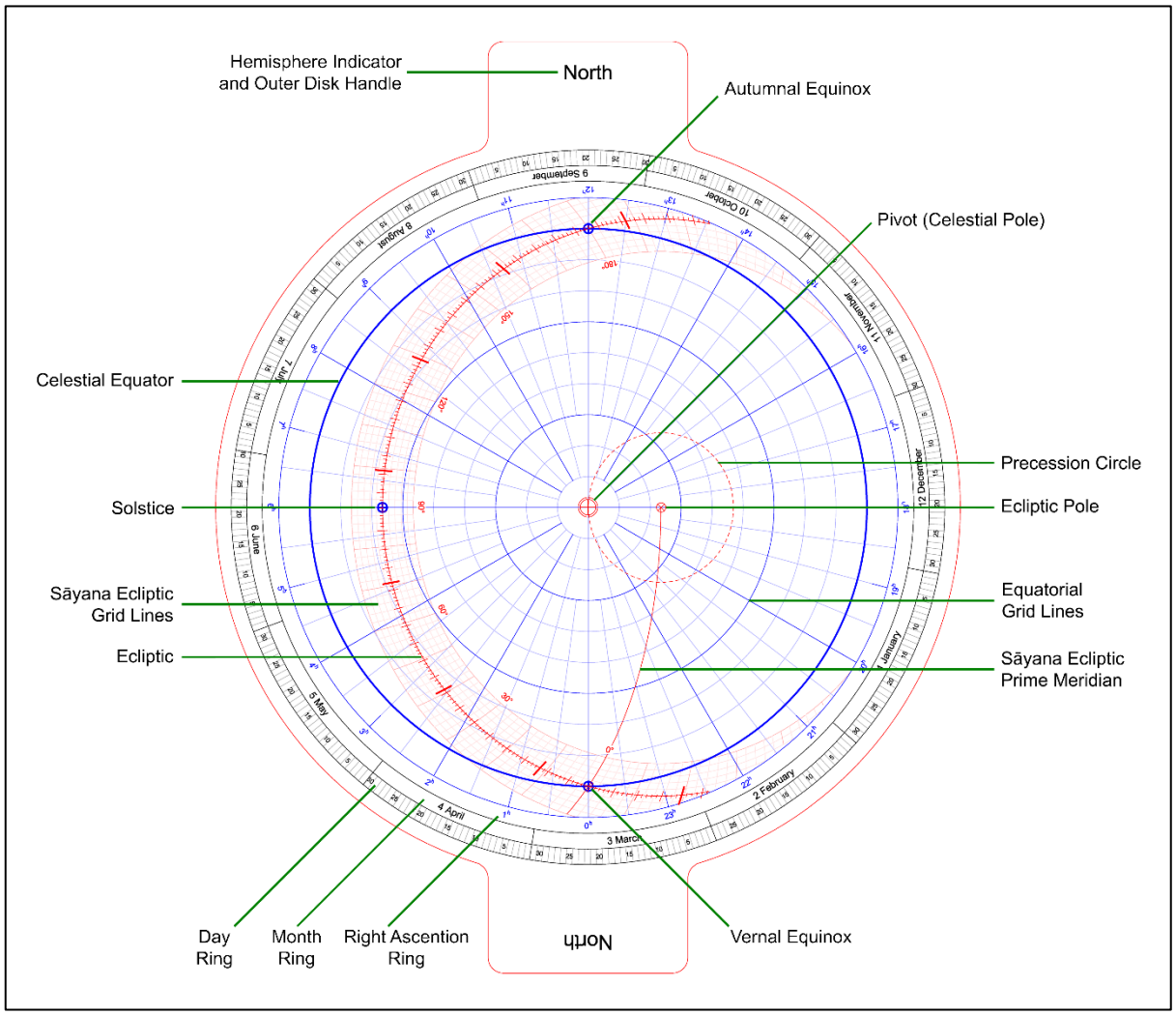


Figure 5: The Northern outer disk of the RP showing the equatorial coordinate grid together with the reduced *sāyana* ecliptic coordinate grid, and a Gregorian calendar ring used to relate stellar positions to calendar date and LMST.

restrial equator, shown as a straight horizontal line through the central pivot, to the horizon at the North Pole. Rising and setting azimuth grids are drawn as non-converging vertical curves perpendicular to the horizon curves and encircling the Eastern and Western points. The horizon at the North and South Poles, which coincides with the celestial equator, is represented by a thick blue circle near the outer edge of the disk.

3.4.5 Equatorial Measurement Scales

An L-shaped group of equatorial measurement scales is provided on the inner disk, analogous in form to the *nirāyana* ecliptic measurement scales on the PP. The declination scale extends from +90° at the NCP and −90° at the SCP at the central pivot to 0° at the celestial equator near the lower edge of the disk. The right ascension minute scale is located along the lower edge of the disk and extends from 0 to 60 minutes. These scales are used in conjunction with the right ascension hour labels on the outer disk to read equatorial coordinates with increased precision. An additional angular scale for reading local mean sidereal time reckoned from the VE is also provided and is positioned opposite the declination scale to maintain visual separation between the two functions.

3.4.6 Time Ring

A circular time ring representing LMST is located at the outermost edge of the inner disk. The ring is marked with hour labels in a 24-hour format. This time ring is used in conjunction with the calendar ring on the outer disk to relate calendar date, time, and horizon phenomena within the RP.

4 RESULTS AND DISCUSSION

This section demonstrates the application of the PP and RP to a series of worked examples drawn from cultural and archaeoastronomical

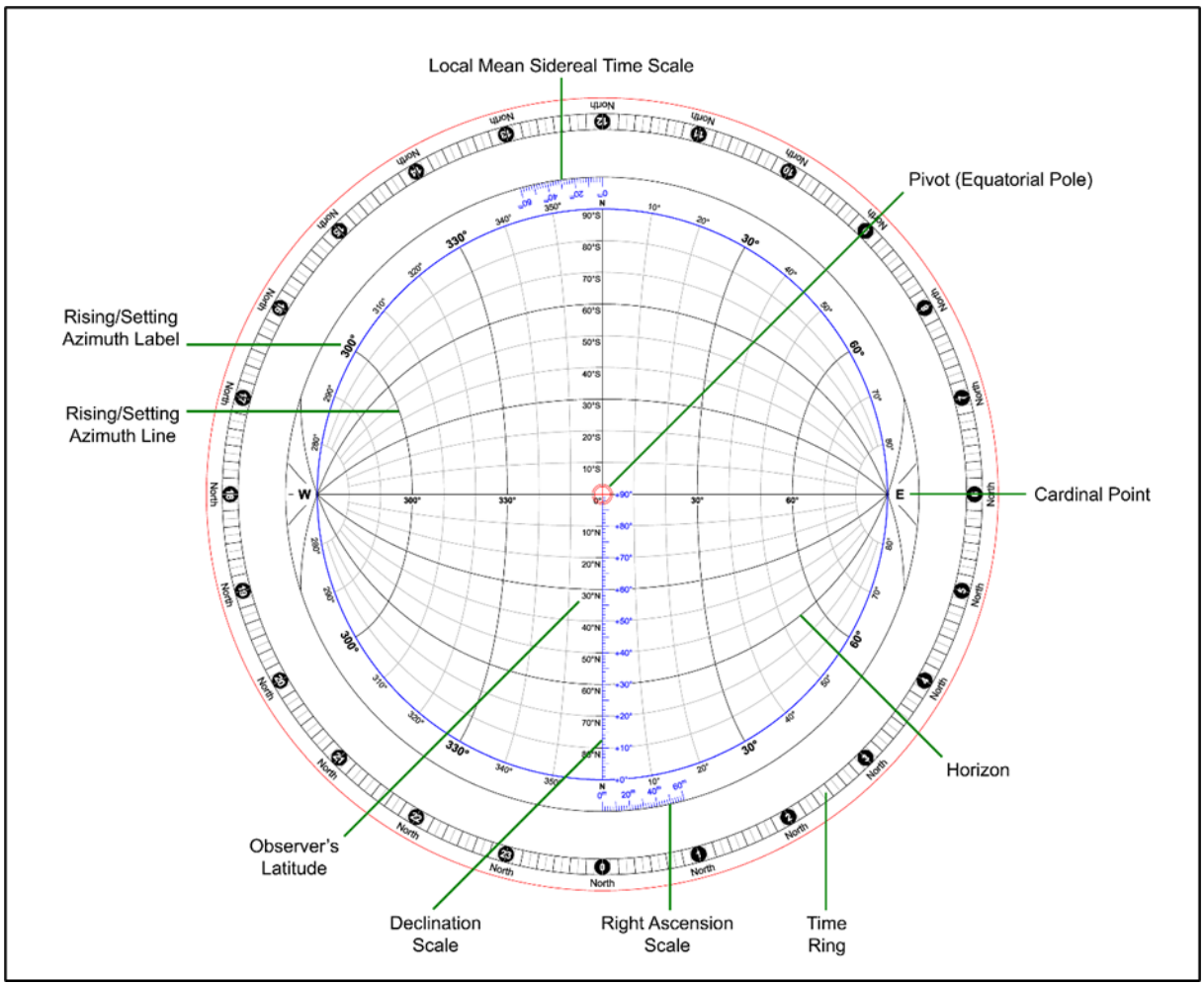


Figure 6: The Northern inner rotating disk of the RP showing the latitude-independent horizontal coordinate grid, equatorial measurement scales, and the LMST ring used to determine rising and setting conditions across different geographic latitudes.

contexts within the exemplar *nirāyana* source system. Rather than introducing new methods, the following subsections present the results obtained by applying the R&R procedure to specific historical dates, geographic locations, and horizon phenomena, and discuss their astronomical and cultural implications. Comparisons with numerically computed results are included to assess consistency and to clarify the scope and limitations of the planispheric approach.

4.1 Azimuth and Time of a Rising or Setting Star at a Given Latitude

This usage describes how the combined primary functions of the PP and RP determine the azimuth, LMST, and local mean sidereal time of the rising or setting of a specific star for a chosen geographic latitude, using only geometric alignment and direct reading from the instruments.

(1) Setting the year on the PP: Select the desired year on the year ring of the outer PP and rotate the inner PP disk until the year indicator points precisely to that year (Figure 7a). This step applies the correct precessional offset.

(2) Reading equatorial coordinates of the Star: The target star is located on the star chart of the outer PP, and its right ascension and declination for the selected year are read directly from the equatorial grid on the inner PP (Figure 7b). This establishes the star's equatorial coordinates of a specified date.

(3) Marking the star on the RP: Using a whiteboard marker, the star's position is plotted on the equatorial coordinate grid on the outer RP by using the right ascension and declination read in step 2. For higher precision, the marking can be refined using the equatorial measurement scales on the inner RP. The outer disk is rotated until the star's right ascension hour value on the outer disk is aligned with its corresponding minute value on the right ascension scale on the inner disk. Then, using the declination scale on the inner disk, the star's declination is located and marked at the corresponding position on the equatorial grid of the outer disk

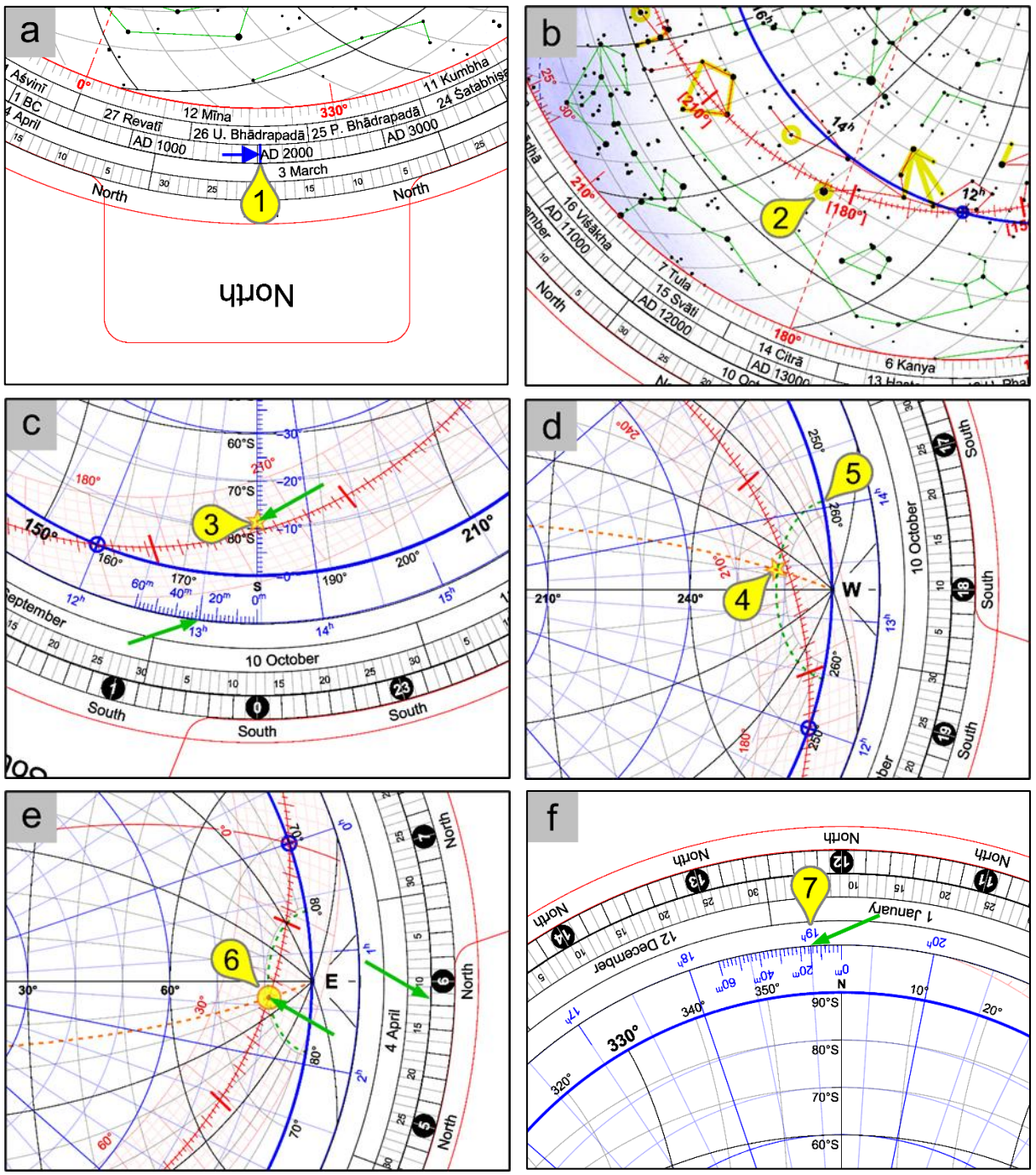


Figure 7: Example of using the PP and RP to find the setting azimuth and time of Spica in 2026 that coincide with sunrise at Phanom Rung in Buriram Province, Thailand (geographic latitude 14.531899° N). Figures a and b show snapshots of the Northern PP, Figures c and d of the Southern RP, and Figures e and f of the Northern RP.

(Figure 7c). This creates a temporary visual reference that can be rotated relative to the horizon grid.

(4) Aligning the star with the horizon: The observer's geographic latitude on the inner RP is located by the corresponding horizon curve. The inner RP disk is rotated until the marked star on the outer disk lies exactly on the Eastern or Western horizon (Figure 7d). This alignment represents the instant of rising or setting.

(5) Reading azimuth and LMST of the star: With this alignment, the rising or setting azimuth is read directly from the horizon azimuth grid lines on the inner disk. Then the LMST of that moment is read with the combination of the calendar ring on the outer disk with the time ring on the inner disk across the edge of the RP (Figure 7d).

(6) Reading azimuth and LMST of the Sun (optional): If the rising or setting phenomenon coincides with the Sun rising or setting, the solar azimuth at the horizon can be found from

the intersection of the ecliptic with the horizon at the given latitude. The date and LMST of these special moments can be read directly using a ruler. A straight line is drawn from the celestial pole (the central pivot) through the point where the ecliptic intersects the horizon. This line indicates the corresponding date on the calendar ring of the outer disk and the LMST on the time ring of the inner disk (Figure 7e).

(7) Reading local mean sidereal time (optional): The local mean sidereal time of the rising or setting phenomenon is determined by combining the right ascension hour label from the outer disk with the minute value read from the local mean sidereal time scale, located opposite to the right ascension measurement scale on the inner disk (Figure 7f).

To better understand this primary usage of the PP and RP, an archaeoastronomical example is given through the orientation of Phanom Rung (latitude 14.531899° N, longitude 102.940175° E). This stone temple complex in Northeastern Thailand was constructed between the tenth and thirteenth centuries on the summit of an extinct volcano and is oriented slightly North of the true East–West axis by about 5.5° (facing azimuth 84.5°). This non-cardinal alignment appears deliberate and has therefore attracted sustained scholarly attention. Identifying the intention behind this orientation is important for clarifying how astronomical knowledge was embedded in religious architecture and how such monuments may have functioned as observational as well as symbolic structures. Previous studies have suggested that the temple was aligned with the star Spica during its acronychal setting at dawn on New Year's Day of the Hindu solar calendar, known as *Meṣa Saṅkrānti*, when the true Sun enters the Indian zodiac sign Aries (Komonjinda et al., 2020).

For AD 2026, this proposal can be examined using the PP and RP. The year 2026 is first set on the PP (Figure 7a), applying the appropriate precessional shift and allowing the equatorial coordinates of Spica to be read from the equatorial grid (Figure 7b). These coordinates are then transferred to the RP and marked on its equatorial coordinate grid (Figure 7c). By drawing the horizon at the latitude of Phanom Rung and rotating the marked position of Spica onto the Western horizon, the azimuth and LMST of its acronychal setting can be read (Figure 7d). From this same configuration, the azimuth, date, and LMST of the rising Sun, together with the corresponding local mean sidereal time, are obtained directly from the RP (Figure 7e).

A comparison between the manually read values obtained from the PP and RP and the numerically computed results from Stellarium version 25.4 shows close agreement across all measured quantities. The equatorial coordinates of Spica for AD 2026 read from the PP are right ascension $13^{h}\ 28^{m}$ and declination −11.5°, compared with the Stellarium values of $13^{h}\ 26^{m}\ 36.42^{s}$ and −11.3°, giving differences of about 0.35° in right ascension and 0.2° in declination. Using these coordinates on the RP for the latitude of Phanom Rung, the acronychal setting azimuth of Spica is read as 258°, while Stellarium gives 258.319°, a difference of roughly 0.3°. The RP yields the corresponding sunrise azimuth of about 80.5° on 12 April 2026 at LMST around 05:53 AM, whereas Stellarium gives the sunrise azimuth of 81.124° on the same date at LMST 05:51:55 AM. At the same moment, the local mean sidereal time read from the RP is $19^{h}\ 15^{m}$, compared with $19^{h}\ 12^{m}\ 36^{s}$ on 12 April 2026 from Stellarium. The rising azimuth difference of about 0.6° and the sidereal time discrepancy of $2^{m}\ 24^{s}$ arise from the simplified Gregorian calendar used in the RP. Taken together, these differences, all within a few tenths of a degree in azimuth and a few minutes in time, indicate strong overall agreement between the manual R&R results and the software-based computations.

4.2 Rising or Setting Star at Given Latitude, Time, and Azimuth

This part describes the reverse process of the previous usage. Instead of starting from a known star and determining its rising or setting conditions, this procedure begins with a specified horizon phenomenon defined by the observer's latitude, LMST, and azimuth, and then determines the equatorial and *nirāyana* ecliptic co-ordinates of the star associated with that phenomenon.

(1) Setting the observer's latitude: The horizon curve on the inner RP corresponding to the given observer's geographic latitude is identified (Figure 8a). This establishes the correct horizon geometry for the selected location.

(2) Setting date and time: The calendar date on the outer disk of the RP is selected and the inner disk rotated until the time ring indicates the specified LMST (Figure 8a). This step fixes the instantaneous orientation of the celestial sphere relative to the observer.

(3) Setting the rising or setting azimuth: On the inner RP, the specified azimuth on the horizon azimuth grid and its intersection with the selected Eastern or Western horizon is identified. This point represents the horizon direction of

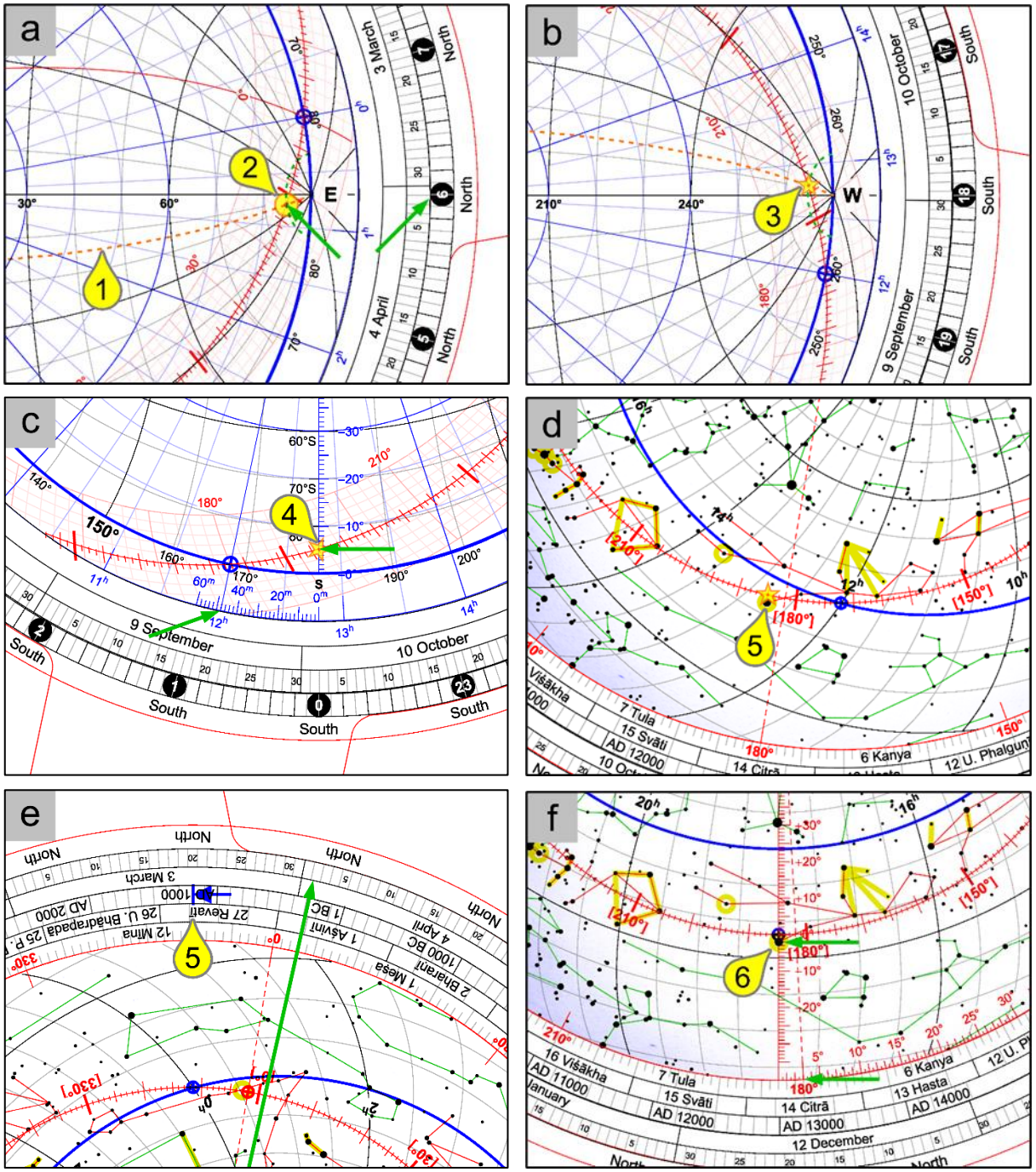


Figure 8: Example of using the PP and RP to identify the acronychal setting star and its epoch at Phanom Rung in Buriram Province, Thailand, given date, time, and azimuth of the star's setting. Figure a shows the snapshot of the Northern RP, Figures b and c of the Southern RP, and Figures d to f of the Northern PP.

of the rising or setting phenomenon and may be marked on the outer disk using a whiteboard marker (Figure 8b).

(4) Reading the equatorial coordinate: The corresponding right ascension and declination is read directly from the equatorial grid lines on the outer RP. Alternatively, the marked star is rotated until it aligns with the declination scale on the inner disk, from which its declination and right ascension values can be read precisely using the equatorial measurement scales (Figure 8c).

(5) Identifying possible star and its epoch: The PP is rotated until the position of the marked star on the RP matches the equatorial coordinate obtained in step 4. The possible star on the outer PP near that position is identified and marked for further reference (Figure 8d). The corresponding epoch is read directly from the year ring on the outer disk, as indicated by the year indicator on the inner disk (Figure 8e).

(6) Reading the *nirāyana* ecliptic coordinate

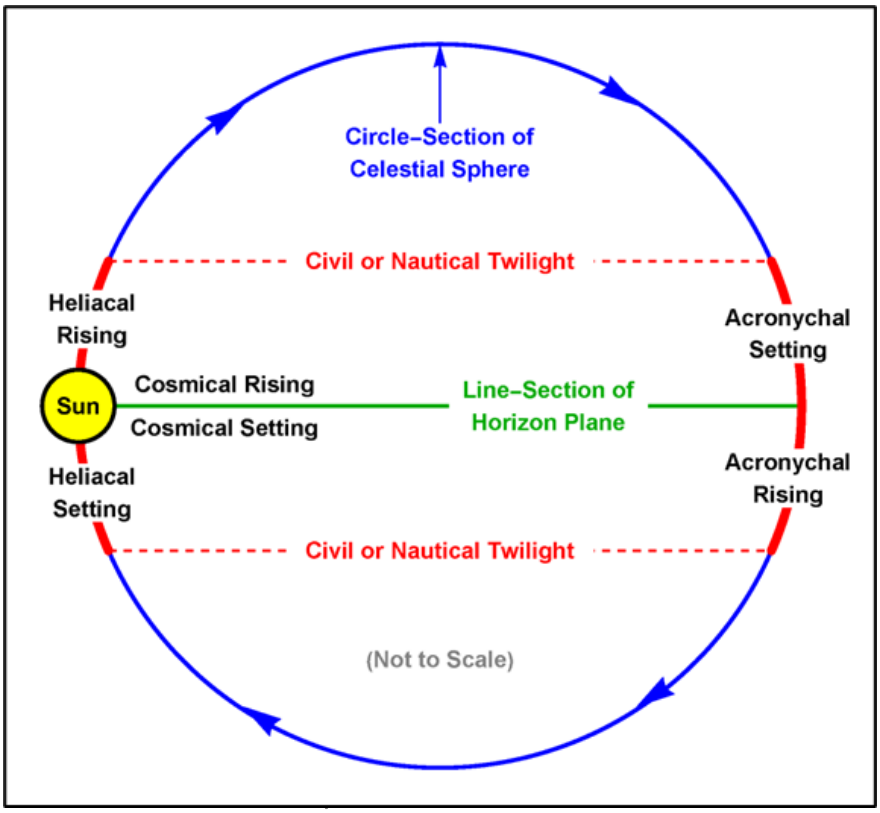


Figure 9. Schematic representation of the classical rising and setting types of a star relative to the Sun and the local horizon. The diagram shows a vertical circle section of the celestial sphere intersecting the horizon plane. Heliacal and acronychal phenomena occur near and opposite the Sun, respectively, within the twilight-limited visibility region, while cosmical rising and setting represent the boundary cases in which the star and the Sun rise or set simultaneously on the horizon.

optional): Once the star is located on the PP, the *nirāyana* ecliptic longitude is read using the *rāśi* and *nakṣatra* rings. Alternatively, more precise *nirāyana* ecliptic longitude and latitude values may be obtained by rotating the marked star to the ecliptic measurement scales (Figure 8f).

(7) Identifying the rising or setting type (optional): Using the calendar date specified in step 2, the position of the marked star is compared with the position of the Sun on the ecliptic as indicated on the PP for that date. The classification of the phenomenon depends on the relative ecliptic longitude of the star with respect to the Sun together with whether the phenomenon identified on the RP is a rising or a setting. Excluding the acronychal rising and setting, which are invisible due to solar glare, the four observable horizon phenomena are as follows (Figure 9).

(a) Heliacal rising: the star is near the Sun and rises shortly before sunrise.

(b) Heliacal setting: the star is near the Sun and sets shortly after sunset.

(c) Acronychal rising: the star lies approximately opposite the Sun and rises near sunset.

(d) Acronychal setting: the star lies approximately opposite the Sun and sets near sunrise.

In the case of Phanom Rung's orientation facing azimuth 84.5°, it has been proposed that this alignment corresponds to the acronychal setting of Spica at the antipodal azimuth of 264.5°, a configuration that Stellarium 25.4 places around 1200 AD and that is also supported by historical evidence (Komonjinda et al., 2020). The PP and RP are suitable for examining this proposal because they jointly address epoch dependent celestial relationships and site specific horizon geometry, allowing the plausibility of the opposed solar and stellar alignment to be assessed geometrically.

On the horizon at Phanom Rung, the position of the rising Sun is first located by rotating the Northern RP to align the ecliptic with azimuth 84.5°, after which the sunrise date and time can be read (Figure 8a). On the Southern side, the opposing setting star on the horizon at azimuth 264.5° can be marked on the outer RP (Figure 8b). Its equatorial coordinate can then be read by rotating this marked star to the equatorial measurement scales (Figure 8c). On the PP, the region corresponding to this coordinate is identified by rotating the planisphere until candidate bright stars appear in that area, and their associated epochs can be read. If the selected star is Spica, the PP is rotated until Spica lies closest to the derived equatorial coordinate (Figure 8d). The epoch is then determined using the year indicator, and it can also be seen that, on the corresponding sunrise date at Phanom Rung, the true ecliptic longitude of the Sun lies directly opposite Spica (Figure 8e). In addition, the *nirāyana* ecliptic coordinate of Spica can be read from the ecliptic measurement scales (Figure 8f).

Using the proleptic Gregorian calendar, the RP gives sunrise at azimuth 84.5° to occur on 2 April at an LMST of about 05:58 AM, whereas in AD 1200 Stellarium gives a sunrise azimuth of 84.562° on 3 April at an LMST of 05:49:40

AM, a one-day difference attributed to the simplified Gregorian Calendar used in the RP. The equatorial coordinates of the antipodal setting star are right ascension $12^h\ 48^m$ and declination −5.0°, for which Stellarium cannot provide a direct value because this position corresponds to a fictitious star. If the physically corresponding star is Spica, the PP indicates that the epoch when its ecliptic longitude is directly opposite that of the Sun on 2 April is around AD 1200. At this same epoch, the PP gives the *nirāyana* ecliptic coordinates of Spica as longitude 183° and latitude −2°, while Stellarium gives a longitude of 182.982° and a latitude of −1.996°, the small difference reflecting the reading resolution of the planispheric scale.

The moment when the Sun rises simultaneously with the setting of Spica corresponds to what is sometimes termed the 'true' acronychal setting of the Spica, a limiting case that is not directly observable to the naked eye because the star disappears at the horizon at the instant of sunrise. In practice, ancient planners would not have relied on this unobservable instant itself, but on the days immediately preceding it. During those days, Spica would have been visible briefly as an 'apparent' acronychal setting, disappearing progressively closer to sunrise (Figure 9). If the true acronychal setting of Spica, which cannot be directly observed, occurred in AD 1200, then the observable apparent acronychal setting would have taken place a few days earlier and at a slightly different azimuth. However, the RP proposed in this study applies only to horizon phenomena under the condition of the true acronychal setting. Therefore, it provides only an approximate date, time, and azimuth. These values are intended as initial estimates and should be refined through further computations if precise results are needed.

This process of identifying the rising or setting star at a given latitude, time, and azimuth is also equivalent to determining the *rāśi* of the *Udaya Lagna*, defined as the intersection point between the ecliptic and the Eastern local horizon. In Hindu astrology, this point is of primary importance because its zodiacal sign, which changes approximately every two hours due to the Earth's rotation, is taken to represent the immediate terrestrial context at the moment of a phenomenon and is used to interpret matters such as personal disposition, auspicious timing, and the suitability of actions undertaken at that instant. The PP and RP can also be applied to determine the *rāśi* of the *Udaya Lagna* with higher geometric fidelity than the approximate formulas traditionally employed in Indian and Southeast Asian astronomical practices, particularly by explicitly accounting for horizon geometry, latitude dependence, and epoch specific celestial orientation.

4.3 *Meṣa Saṅkrānti* and New Year's Day at a Given Year

In Thailand, the traditional Songkran Festival is observed over three consecutive days: (1) *Wan Songkran*, marking the moment of *Meṣa Saṅkrānti* when the true Sun enters Aries, (2) *Wan Nao*, the transitional day between the old and new year, and (3) *Wan Thaloeng Sok*, the official New Year's Day in the traditional Thai Mahasakaraj calendar. The duration and interpretation of these observances are shaped by local calendrical practice rather than a universal cultural rule. Within the Thai context, the three-day structure may be examined astronomically through the distinction between the true and mean solar motion, since the true Sun reaches Aries approximately two days before the mean Sun. This framework illustrates how the dual planispheres can be applied to investigate the relationship between observational astronomy, calendrical reckoning, and locally defined ritual timing.

In Hindu astronomy, *Meṣa Saṅkrānti* is traditionally reckoned using LMST at the prime meridian of Ujjayini in present-day India. In contrast, the Thai traditional calendar defines *Wan Thaloeng Sok* as the entry of the geocentric mean Sun into Aries. Although these phenomena occur simultaneously worldwide, the true and mean Sun differ in ecliptic longitude, a distinction well-documented in Indian and Southeast Asian astronomical treatises. Modern computation using the Equation of the Center shows that this difference at the Meṣa *Saṅkrānti* moment is about 1.89°, corresponding to roughly two days of the Sun's movement on the ecliptic. Consequently, the true Sun reaches Aries about two days before the mean Sun, which may explain why the Hindu New Year festival spans three days in Thailand.

The PP can also be used to determine the timing of this three-day festival by rotating it to the desired year. At present, the PP indicates that the New Year festival in AD 2026 falls between 11 and 13 April (Figure 10a), whereas calculations based on the Thai *Suriyayatra-Manat* treatise place the Songkran festival between 14 and 16 April. This three-day discrepancy arises from differences in the adopted length of the sidereal year reckoned from the FPA. The *Suriyayatra-Manat* uses a value of 365.25875 mean solar days, while the modern value is 365.256363 mean solar days. The resulting difference of 206.2368 seconds per year accumulates to approximately 3.64 days be-

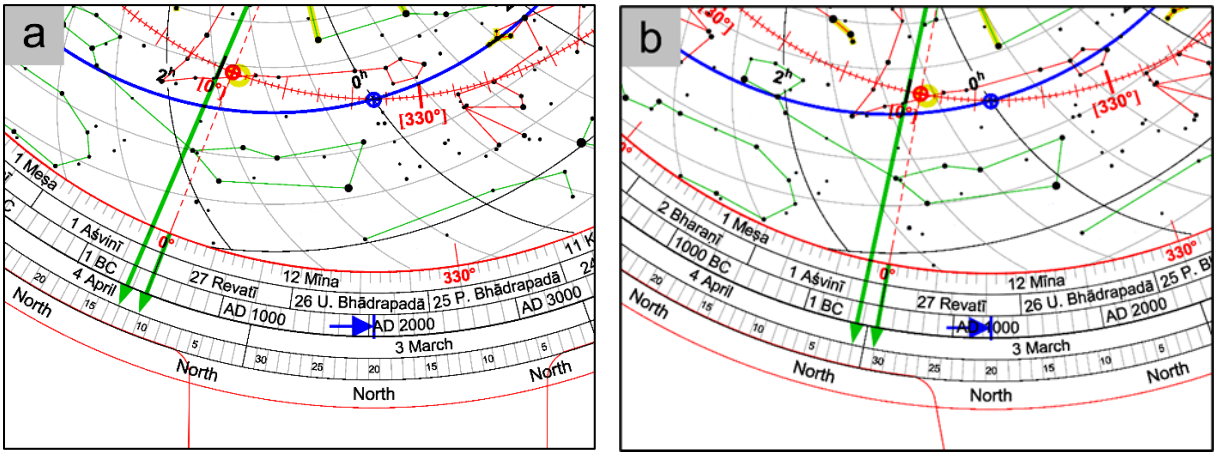


Figure 10: Example of using the PP to estimate the true date of the New Year festival from the Sun's true and mean *nirāyana* ecliptic longitude. Both positions of the Sun are plotted on the ecliptic and can be used to identify the date of *Meṣa Saṅkrānti* and the corresponding festival dates for the selected year.

tween AD 500 and AD 2026, accounting for the observed delay of the New Year festival relative to the astronomical date.

Using the same discrepancy-accumulation procedure, the dates of the New Year festival predicted by the *Suriyayatra-Manat* can be estimated for any chosen year. For example, by AD 1250 the difference accumulates over 750 years to about 1.79 days. The PP therefore places the true *Meṣa Saṅkrānti* on 31 March and *Wan Thaloeng Sok* on 2 April (Figure 10b). In contrast, the *Suriyayatra-Manat* would shift these dates later by approximately 1.79 days, to about 1 April and 3 April, respectively. This method allows historical researchers to reconstruct how traditional calendar dates shifted over time and compare them with archaeological or textual evidence.

Another Hindu New Year's observance is *Makara Saṅkrānti* (also known as *Mahā Saṅkrānti*), which is now typically celebrated on 14 January. It is defined as the moment when the Sun enters the Indian zodiac sign *Makara* (the Western zodiac sign Capricorn) and is said to coincide with the Winter Solstice (WS). However, the WS occurs in late December each year, not in January, as *Mahā Saṅkrānti* does. This mismatch suggests that linking *Mahā Saṅkrānti* to the WS may reflect the historical period when that definition was established (Vedanidhi Sangmek, personal communication, 11 January 2026). This epoch can be readily determined using the PP.

To identify this epoch the PP is rotated to AD 2026 and 14 January is located. With a ruler, the Sun's exact position on the ecliptic on the outer PP is marked (Figure 11a). The PP is then rotated until this marked position aligns with the WS on the inner PP, and the corresponding year at the year indicator is read (Figure 11b). This R&R transformation indicates an origin epoch of roughly AD 100, when Stellarium likewise shows that the Sun's position at the WS relative to nearby stars is very close to that marked on the PP. This agreement suggests that the PP can be used to recover the historical timeframe in which *Mahā Saṅkrānti* was originally aligned with the Winter Solstice.

4.4 Accuracy and Uncertainty

The accuracy of the dual planisphere is primarily limited by the finite resolution of the printed scales and the practical ability to interpolate between tick marks. To provide an instrument-only estimate of accuracy (without user-sampling trials), the uncertainty associated with each reading was treated as a quantization error with step size Δ. Assuming the true value lies uniformly within the interval $[-\Delta/2, +\Delta/2]$, the maximum absolute error is bounded by $\pm\Delta/2$, while the corresponding standard uncertainty is $u = \Delta/\mathrm{sqrt}(12)$, with an expanded uncertainty (approximately 95% coverage) given by $U \approx 2u = \Delta/\mathrm{sqrt}(3)$. Table 3 summarizes the adopted scale resolutions and the associated uncertainties for the main quantities read from the planisphere.

While the ecliptic latitude or declination uncertainty remains largely controlled by the corresponding scale resolution, the effective accuracy of derived quantities such as ecliptic longitude and right ascension is not uniform over the sphere. As the ecliptic latitude or declination approaches the pole, the geometry becomes increasingly sensitive because lines of constant longitude and constant right ascension converge. Consequently, their fixed reading uncertainties or small differences in alignment when transferring positions between rings, can produce a comparatively larger change in the inferred ecliptic longitude or right ascension (and

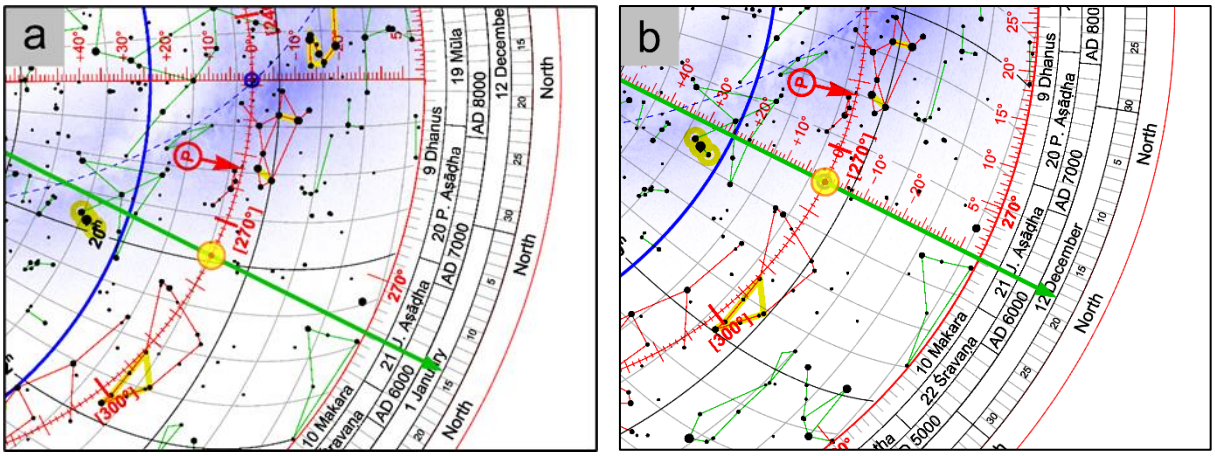


Figure 11: Example of using the PP to estimate the epoch when *Mahā Saṅkrānti* coincided with the historical WS by marking the Sun's position on 14 January (AD 2026) and rotating it to align with the WS point, giving an epoch of approximately AD 100.

Table 3: Scale-resolution-based uncertainty estimates for the dual planisphere readings.

Quantity	Step Size Δ	Max Error ±Δ/2	Standard Uncertainty u = Δ/sqrt(12)	Expanded Uncertainty U = Δ/sqrt(3)
Ecliptic Longitude	0.5°	0.25°	0.144°	0.289°
Ecliptic Latitude and Declination	1°	0.5°	0.289°	0.577°
Right Ascension and Local Mean Sidereal Time	2 min (0.5°)	1.0 min (0.25°)	0.577 min (0.144°)	1.155 min (0.289°)
Local Mean Solar Time (LMST)	5 min	2.5 min	1.443 min	2.887 min
Calendar Date	1 day	0.5 day	0.289 day	0.577 day
Year	100 years	50 years	28.87 years	57.74 years

hence the local mean sidereal time) at high ecliptic latitudes or declinations. This effect should be expected to increase scatter for near-polar objects even when the underlying printed scale resolution is unchanged.

5 CONCLUDING REMARKS

This study has presented a dual planispheric system composed of the PP and RP as a means of extending the analytical scope of traditional planispheric instruments across wider temporal and geographic contexts. By separating celestial transformation into two coordinated analog devices, the proposed framework addresses the geometric limitations inherent in single-planisphere designs while maintaining direct visual correspondence between celestial coordinate systems and observable horizon phenomena. The PP isolates long-term axial precession within an ecliptic-to-equatorial transformation, while the RP performs the equatorial-to-horizontal transformation independently of fixed latitude. Together, this division preserves conceptual transparency while enabling systematic comparison of sky configurations across millennial-scale timespans and geographically diverse observing locations.

Applications of the PP and RP demonstrate that horizon-related astronomical phenomena can be examined coherently without recourse to numerical computation. Through the rotate-and-read workflow, rising and setting behavior, azimuthal alignment, and time-dependent relationships emerge directly from geometric alignment rather than algorithmic calculation. The worked examples show that classical categories of stellar phenomena are not merely historical conventions but arise naturally from the spatial relationships among the Sun, stars, and the local horizon. When applied to cultural and architectural contexts, the instruments support the reconstruction of calendrical practices, ritual timing, and monument orientation grounded in observation-based astronomy. The close agreement between planispheric readings and modern software simulations indicates that simplified analog representations remain analytically meaningful even within contemporary research environments.

Beyond the specific case studies presented, the dual planispheres provide a transparent framework for investigating long-term celestial change and the evolution of astronomy-based traditions. The instruments allow researchers to visualize precessional drift, shifts in calendrical reference points, and the interaction between true and mean solar motion within historically grounded coordinate systems. By making co-

ordinate transformation physically observable, the planispheres reveal assumptions that are often obscured in purely computation-based approaches and encourage cross-cultural comparative study. In this respect, the system contributes not only to the reconstruction of historical practice but also to the development of a reproducible, method-based bridge linking material culture, geometric reasoning, and modern archaeoastronomical analysis.

Equally important is the pedagogical potential of the PP and RP. Because celestial mechanics are explored through embodied, hands-on manipulation rather than abstract computation, users can directly experience the geometric logic underlying precession, sidereal time, and horizon transformation. Such interaction supports intuitive understanding for learners with varied levels of mathematical preparation and offers opportunities for integration into secondary-school teaching, undergraduate astronomy courses, museum exhibitions, and heritage-based educational programs. The instruments illustrate how historically informed, hands-on approaches can complement contemporary digital visualization and AI-driven tools by making underlying transformations visible, interpretable, and conceptually grounded. Although not intended for high-precision measurement, their schematic and interaction-based character promotes conceptual clarity, reinforcing the enduring educational value of analog astronomical instruments in both research and modern science education.

6 ACKNOWLEDGEMENTS

This study was supported by the National Research Council of Thailand (NRCT) [Grant No. N91A690609]. It is also part of the archaeoastronomy collaboration between the National Astronomical Research Institute of Thailand (NARIT) and Walailak University. Dual planispheres in this study were inspired by *The Astrolabe* by J.E. Morrison, kindly provided by Kanatawan Aungsakul, as well as by the precession planisphere developed by Dr. Dominic Ford. The authors also thank Dr. Siramas Komonjinda and Korakamon Sriboonrueang for their archaeoastronomical research on Phanom Rung's orientation.

Portions of this work were previously presented under the title "Generalized Planispheres for Archaeoastronomical Research" at the 22nd Indo-Pacific Prehistory Association (IPPA) Conference, held from 6 to 12 November 2022 in Chiang Mai, Thailand. The PP has been registered as a petty patent under the title "Planisphere in Ecliptic–Equatorial Coordinate System" (แผนที่ดาวแบบหมุนระบบพิกัดสุริยวิถี–ศูนย์สูตรฟ้า, in Thai), issued by Thailand's Department of Intellectual Property (DIP) on 11 May 2023 (Petty Patent No. 21573). The RP has likewise been registered as a petty patent under the title "Latitude-Independent Stellar Rising and Setting Planisphere" (แผนที่การขึ้นตกของดาวที่ไม่ขึ้นกับละติจูดผู้สังเกตการณ์, in Thai), issued by Thailand's DIP on 2 December 2024 (Petty Patent No. 24889).

7 REFERENCES

Aterini, B., 2019. Geometric instruments for the orientation and measurement: the astrolabes. *Advances in Historical Studies*, 8(1), 58–78 (https://doi.org/10.4236/ahs.2019.81004).

Bentley, P., 2018. Star taker: art, science and mathematics in an astrolabe from fourteenth-century Spain. *Journal of Mathematics and the Arts*, 12(2–3), 170–180 (https://doi.org/10.1080/17513472.2018.1477037).

Bizouard, C., and Cheng, Y., 2023. The use of the quaternions for describing the Earth's rotation. *Journal of Geodesy*, 97, Article 53 (https://doi.org/10.1007/s00190-023-01735-z).

Burgess, E., 1935. *Translation of the Sūrya-Siddhānta: A Textbook of Hindu Astronomy, With Notes and An Appendix*. Calcutta, University of Calcutta.

Calabretta, M.R., and Greisen, E.W., 2002. Representations of celestial coordinates in FITS. *Astronomy & Astrophysics*, 395(3), 1077–1122 (https://doi.org/10.1051/0004-6361:20021327).

Capitaine, N., Wallace, P.T., and Chapront, J., 2003. Expressions for IAU 2000 precession quantities. *Astronomy & Astrophysics*, 412(2), 567–586 (https://doi.org/10.1051/0004-6361:20031539).

Capitaine, N., and Wallace, P.T., 2006. High-precision methods for locating the celestial intermediate pole and origin. *Astronomy & Astrophysics*, 450(3), 855–872 (https://doi.org/10.1051/0004-6361:20054550).

Castro, F., Budsberg, N., Jobling, J., and Passen, A., 2015. The astrolabe project. *Journal of Maritime Archaeology*, 10, 205–234 (https://doi.org/10.1007/s11457-015-9149-9).

Davis, J.F., and Lowne, M., 2015. An early English astrolabe at Gonville & Caius College, Cambridge, and Walter of Elveden's Kalendarium. *Journal for the History of Astronomy*, 46(3), 257–290 (https://doi.org/10.1177/0021828615590336).

Finney, B., 2001. Navigation. In Smelser, N.J., and Baltes, P.B. (eds.), *International Encyclopedia of the Social & Behavioral Sciences*. Amsterdam, Elsevier. Pp. 10410–10413 (https://doi.org/10.1016/b0-08-043076-7/00922-0).

Gessner, S., 2024. 'Si te omnimoda delectat precisio': Early astronomical instruments with scales and the multiple meanings of precision in the sixteenth century. *Annals of Science*, 81(1–2), 30–59 (https://doi.org/10.1080/00033790.2023.2285845).

Gislén, L., and Evans, J., 2024. The artful early instruments of Peter Apian: Ein kunstlich Instrument of 1524, its

precursors and its successors. *Journal for the History of Astronomy*, 55(2), 207–278 (https://doi.org/10.1177/00218286241241070).
International Astronomical Union. 2022. *The constellations*. IAU Archive (https://iauarchive.eso.org/public/themes/constellations/; accessed 1 January 2026).
Jenkins, A., 2013. The Sun's position in the sky. *European Journal of Physics*, 34(3), 633–652 (https://doi.org/10.1088/0143-0807/34/3/633).
Jones, A., 2015. Transmission of Babylonian astronomy to other cultures. In Ruggles, C.L.N. (ed.), *Handbook of Archaeoastronomy and Ethnoastronomy.* New York, Springer. Pp. 1877–1881 (https://doi.org/10.1007/978-1-4614-6141-8_194).
King, D.A., 2019. European astrolabes to ca. 1500: an ordered list. In Rodríguez-Arribas, J., Burnett, C., Ackermann, S., and Szpiech, R. (eds.), *Astrolabes in Medieval Cultures.* Leiden, Brill. Pp. 357–366 (https://doi.org/10.1163/9789004387867_013).
Koad, P., Riyaprao, O., Saelee, C., and Chaisriya, K., 2025. Dating Srivijaya inscriptions: utilizing modern computations in archaeoastronomy. *Journal of Astronomical History and Heritage*, 28(3), 586–611 (https://doi.org/10.3724/sp.j.1440-2807.2025.03.04).
Komonjinda, S., Riyaprao, O., Sriboonrueang, K., and Saelee, C., 2021. Relative orientation of Prasat Hin Phanom Rung temple to Spica on New Year's Day: The chief indicator for the intercalary year of the luni-solar calendar. *Proceedings of the International Astronomical Union*, *15*(S367), 260–264 (https://doi.org/10.1017/s1743921321001034).
Liu, Z., Li, C., Zhang, C., Tong, S., Chen, Z., Lu, H., Zhang, X., and Yang, Y., 2022. Optimum geometric distribution of stellar observations in astronomical positioning. *Journal of Surveying Engineering*, 149(1), Article 04022017 (https://doi.org/10.1061/(asce)su.1943-5428.0000414).
Longair, M., 2021. James Croll, celestial mechanics and climate change. *Earth and Environmental Science Transactions of the Royal Society of Edinburgh*, 112(3–4), 231–238 (https://doi.org/10.1017/s1755691021000165).
McCluskey, S.C. 2015. Astronomy in the service of Christianity. In Ruggles, C.L.N. (ed.), *Handbook of Archaeoastronomy and Ethnoastronomy*. New York, Springer. Pp. 165–179 (https://doi.org/10.1007/978-1-4614-6141-8_15).
Morris, B.M., Tollerud, E., Sipőcz, B., Deil, C., Douglas, S.T., plus 7 further authors, 2018. Astroplan: an open source observation planning package in Python. *The Astronomical Journal*, 155(3), Article 128 (https://doi.org/10.3847/1538-3881/aaa47e).
Morrison, J.E., 2007. *The Astrolabe*. Rehoboth Beach, Janus.
Morrison, R.G., 2013. Islamic astronomy. In Lindberg, D.C., and Shank, M.H. (eds.), *The Cambridge History of Science: Volume 2, Medieval Science*. Cambridge, Cambridge University Press. Pp. 109–138.
Moyer, A., 1999. The astronomers' game: astrology and university culture in the fifteenth and sixteenth centuries. *Early Science and Medicine*, 4(3), 228–250 (https://doi.org/10.1163/157338299x00157).
Müller, W.H., 2015. The spin, the nutation, and the precession of the Earth's axis revisited from a (numerical) mechanics perspective. *Journal of Applied Mathematics and Mechanics*, 95(10), 992–1003 (https://doi.org/10.1002/zamm.201400252).
Myers, J.R., Sande, C.B., Miller, A.C., Warren, W.H., Jr., and Tracewell, D.A., 2015. *SKY2000 Master Catalog, Version 5, Revision 4* (VizieR Online Data Catalog: V/145). Centre de Données Astronomiques de Strasbourg (https://cdsarc.cds.unistra.fr/viz-bin/cat/V/145; accessed 1 January 2026).
Nothaft, C.P.E., 2017. Criticism of trepidation models and advocacy of uniform precession in Medieval Latin astronomy. *Archive for History of Exact Sciences*, 71, 211–244 (https://doi.org/10.1007/s00407-016-0184-1).
Pai, R.V., and Shylaja, B.S., 2016. Measurement of coordinates of *Naksatras* in Indian astronomy. *Current Science*, 111(9), 1551–1558.
Riyaprao, O., Sriboonrueang, K., Komonjinda, S., and Saelee, C., 2023. The astronomical orientation of the Thai Phra That Doi Suthep temple in relation to the acronychal rising of Alpha Corona Borealis and Visakha Bucha Day. *Journal of Astronomical History and Heritage*, 26(3), 701–721 (https://doi.org/10.3724/sp.j.1440-2807.2023.09.68).
Safiai, M.H., Ibrahim, I.A., Jamsari, E.A., Nasir, B.M., and Ahmad, M.Y., 2017. Astrolabe as portal to the Universe: inventions across civilizations. *International Journal of Civil Engineering and Technology*, 8(11), 609–619.
Sastri, S.D., 1931. *Vedānga Jyotiṣa of Lagadha: With translation and Notes*. Pune, Bhandarkar Oriental Research Institute.
Seidelmann, P.K., and Gurfil, P., 2016. *Celestial Mechanics and Astrodynamics: Theory and Practice*. Springer (https://doi.org/10.1007/978-3-662-50370-6).
Smith, B.S., 2002. An astrolabe from Passa Pau, Cape Verde Islands. *International Journal of Nautical Archaeology*, 31(1), 99–107 (https://doi.org/10.1111/j.1095-9270.2002.tb01404.x).
Strano, G., 2017. A new approach to the star data of early planispheric astrolabes. *Medieval Encounters*, 23(1–5), 444–467 (https://doi.org/10.1163/15700674-12342255).
Warren, W.H., Jr., 2001. *Analysis and Quality Assurance of the SKYMAP 4.0 Guidance and Tracking Star Catalog: The NASA SKY2000 Spacecraft Altitude Determination Star Catalog* (Report No. RTSC-3447). NASA Goddard Space Flight Center (https://ntrs.nasa.gov/citations/20010066140; accessed 1 January 2026).
Zotti, G., 2008. Tangible heritage: production of astrolabes on a laser engraver. *Computer Graphics Forum*, 27(8), 2169–2177 (https://doi.org/10.1111/j.1467-8659.2008.01193.x).
Zotti, G., Hoffmann, S.M., Wolf, A., Chéreau, F., and Chéreau, G., 2021. The simulated sky: Stellarium for cultural astronomy research. *Journal for Skyscape Archaeology,* 6(2), 221–258 (https://doi.org/10.1558/jsa.17822).



Dr. Peeravit Koad was born in Ranong, Thailand in 1992. He completed a PhD in Computational Science at Walailak University, Nakhon Si Thammarat, Thailand. He also received scholarships from the Junior Science Talent Project under the National Science and Technology Development Agency.

He is interested in science, technology, and innovation, especially in multi-paradigm data science and artificial intelligence, which can be applied in many fields that require statistical data analysis, such as geoinformatics, climatology, and astronomy.

Peeravit's current research project focuses on the geographical history of the Thai–Malay Peninsula that can push the boundary of its history back 2000 years or more into the Suvarṇabhūmi Period.



Dr. Kannattha Chaisriya was born in Phatthalung (Thailand) in 1980. She received a PhD in Computer Science from the University of Southampton, United Kingdom, in 2016. She is a lecturer in the Interactive Multimedia Animation and Game Program, School of Informatics, Walailak University, Nakhon Si Thammarat, Thailand.

Her expertise includes research in the fields of 3D graphics, digital games, digital cultural heritage, multimedia technology, mobile applications, and web technology.



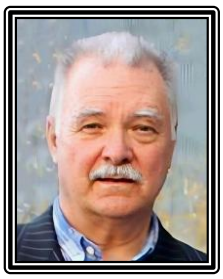
Orapin Riyaprao was born in Chiang Rai (Thailand) in 1976. She has a BS in Statistics from Chiang Mai University (Chiang Mai, Thailand) and an MA in Applied Mathematics from Long Island University (New York, USA). Currently she is a Specialist and heads the History and Heritage of Astronomy group at the National Astronomical Research Institute of Thailand in Chiang Mai. Formerly she worked as a lecturer in the School of Science, Mae Fah Luang University in Chiang Rai, Thailand.

For the past 12 years, Orapin's research interests have included Lanna and Thai historical records; the history of Indian, Chinese, Burmese and Thai calendars; temple orientations with respect to the azimuth of sunrise–sunset; and the wisdom of astronomy in Lanna Culture and its related kingdoms (i.e. the Kingdoms of Hariphunchai, Sukhothai, Ayutthaya, Lavo, Pagan, and Angkor).

Dr. Cherdsak Saelee was born in Chiang Mai (Thailand) in 1970. He has BS (First Class Honours) and MS degrees from Chiang Mai University, and a PhD in Physics (in 1999) from Leeds University in the UK. Since 1995 he has worked as a lecturer in the Department of Physics and Materials Science at Chiang Mai University.



For more than two decades he has been interested in archaeoastronomy as well as the Thai calendar, particularly in relation to Northern Thailand. His archaeo-astronomical research is an extension of the research conducted by the late Associate Professor Samai Yodinthara, Assistant Professor Mullika Thavornathivas, and Associate Professor Sanan Supasai, all three of whom had been researching and gathering information for more than 30 years. Cherdsak has collaborated with them since 1990 in three major areas: an outreach project to unify teaching and learning concepts for teachers and schools in Thailand; the relationship between the orientation of monastery temples and associated cultural traditions; and the Thai lunar calendar.



Lester Gilbert was born in 1950 in southern Africa. He has an MSc from the University of Cape Town. After a number of academic and industrial positions in Africa and the UK, he was an Associate Professor in the School of Engineering and Computer Science at the University of Southampton (UK) where he was appointed as an Emeritus Fellow upon retirement.

Lester's publications are mainly centered on the use of computers in learning and teaching, with extensive collaboration on doctoral and post-doctoral research studies with colleagues in Southeast Asia.